AIRBORNE MEASUREMENTS OF OPTICAL ATMOSPHERIC PROPERTIES SUMMARY AND REVIEW II

Seibert Q. Duntley, Richard W. Johnson, and Jacqueline I. Gordon

Visibility Laboratory
University of California, San Diego
Scripps Institution of Oceanography
San Diego, California 92152

Approved:

S. Q. Duntley

Seibert Q. Duntley, Director
Visibility Laboratory

Approved:

William A. Nierenberg

William A. Nierenberg, Director
Scripps Institution of Oceanography

CONTRACT NO. F19628-73-C-0013
Project No. 7621
Task No. 762104
Work Unit No. 76210401

Final Report
1 September 1972 – 31 July 1975

Contract Monitor: Maj. R. W. Endlich, Optical Physics Laboratory

Prepared for

AIR FORCE CAMBRIDGE RESEARCH LABORATORIES
AIR FORCE SYSTEMS COMMAND
UNITED STATES AIR FORCE
HANSCOM AFB, MASSACHUSETTS 01731

UNCLASSIFIED

SECURITY CLASSIFICATION OF THIS PAGE *(When Data Entered)*

REPORT DOCUMENTATION PAGE

READ INSTRUCTIONS BEFORE COMPLETING FORM

1. REPORT NUMBER: AFCRL-TR-75-0457	2. GOVT ACCESSION NO.
3. RECIPIENT'S CATALOG NUMBER	
4. TITLE *(and Subtitle)*: AIRBORNE MEASUREMENTS OF OPTICAL ATMOSPHERIC PROPERTIES, SUMMARY AND REVIEW II	5. TYPE OF REPORT & PERIOD COVERED: Final Report, 1 September 1972 – 31 July 1975
	6. PERFORMING ORG. REPORT NUMBER: SIO Ref. 75-26
7. AUTHOR(s): Seibert Q. Duntley, Richard W. Johnson, Jacqueline I. Gordon	8. CONTRACT OR GRANT NUMBER(s): F19628-73-C-0013
9. PERFORMING ORGANIZATION NAME AND ADDRESS: Visibility Laboratory, University of California, San Diego, Scripps Institution of Oceanography, San Diego, California 92152	10. PROGRAM ELEMENT, PROJECT, TASK AREA & WORK UNIT NUMBERS: 76210401, 62101F
11. CONTROLLING OFFICE NAME AND ADDRESS: Air Force Cambridge Research Laboratories, Hanscom AFB, Massachusetts 01731, Contract Monitor/OPA/Maj. R. Endlich	12. REPORT DATE: September 1975
	13. NUMBER OF PAGES: 85
14. MONITORING AGENCY NAME & ADDRESS *(if different from Controlling Office)*	15. SECURITY CLASS. *(of this report)*: UNCLASSIFIED
	15a. DECLASSIFICATION/DOWNGRADING SCHEDULE

16. DISTRIBUTION STATEMENT *(of this Report)*

Approved for public release, distribution unlimited.

17. DISTRIBUTION STATEMENT *(of the abstract entered in Block 20, if different from Report)*

18. SUPPLEMENTARY NOTES

19. KEY WORDS *(Continue on reverse side if necessary and identify by block number)*

Atmospheric Optical Properties	Atmospheric Contrast Transmittance	Daytime Irradiance
Atmospheric Scattering Coefficient	Atmospheric Path Reflectance	Terrain Reflectance
Atmospheric Beam Transmittance	Daytime Radiance	Radiometry

20. ABSTRACT *(Continue on reverse side if necessary and identify by block number)*

This report summarizes a 3-year period of collecting optical atmospheric data both at night and during the day chiefly with airborne instruments. Four field expeditions were made between September 1972 and June 1975 in various locations in the United States and Europe, primarily during the winter and summer. Measurements were made in five spectral regions, as follows: three narrow band optical filters with mean wavelengths of 478, 664, and 765 nanometers, and two broad band sensitivities, one representing the S-20 multiplier phototube incorporating an ultraviolet rejection filter with a mean wavelength of 532 nanometers, the other representing the photopic response with a mean wavelength

DD FORM 1 JAN 73 1473 EDITION OF 1 NOV 65 IS OBSOLETE
S/N 0102-014-6601

UNCLASSIFIED

SECURITY CLASSIFICATION OF THIS PAGE *(When Data Entered)*

Block 20 cont.

of 557 nanometers. Optical measurements included total scattering coefficient and sky and terrain radiance. These data were used to calculate natural irradiance on a horizontal plane surface, directional reflectance of terrain, atmospheric beam transmittance, path radiance, and directional path reflectance. The methods of data collection and data processing are reviewed, the resultant data bank described, and recommendations for further study and interpretation of the data are proposed.

SUMMARY

This is the final report prepared in compliance with AFCRL Contract F19628-73-C-0013. The principal tasks under this contract were (1) to perform a series of missions to collect atmospheric optical data in various locations in the United States and Europe, (2) to build a ground-based variable path function meter similar to the wingtip path function meter used on the C-130 aircraft, and (3) to modify the airborne integrating nephelometer so that it would fit inside a C-130H upper radome. The purpose of the data measurements was to determine several important optical properties of various downward-inclined paths of sight. These properties include the natural irradiance upon horizontal plane surfaces, scalar irradiances, total volume scattering coefficients, atmospheric beam transmittances, directional path reflectances, directional terrain reflectances, and path radiances.

Four field trips were made. Data from the fourth field trip, which was to western Washington, have been issued as Scientific Report 5 [AFCRL-TR-75-0414, Duntley, *et al.* (1975]. In addition, two sets of data collected during a previous contract interval were issued as Scientific Reports 3 and 4 [AFCRL-TR-73-0422 and AFCRL-TR-74-0298, Duntley, *et al.* (1973 and 1974)]. The status of the total data bank resulting from the 3-year period is reviewed in this report.

The instrumentation developed at the Visibility Laboratory and mounted in Air Force C-130A, aircraft No. 50022, consisted of a total scattering meter (or integrating nephelometer) for determining the total scattering coefficient, two sky scanning radiometers for recording upper and lower sky radiances, a dual irradiometer for recording alternately the downwelling and upwelling irradiances upon horizontal plane surfaces, an equilibrium radiance telephotometer, and a variable direction path function meter. The meteorological instrumentation included a Royco particle counter, pressure transducers, a dewpoint hygrometer, and an AN/AMQ-17 aerograph for measuring ambient temperature and humidity.

Each optical instrument was fitted with five optical filters causing it to measure at three narrow band wavelengths of the spectrum and two broad pass bands as follows: three narrow band filters at mean wavelengths of 478, 664, and 765 nanometers, a filter representing the photopic response with a mean wavelength of 557 nanometers, and one with a mean wavelength of 532 nanometers representing the S-20 multiplier phototube with an ultraviolet rejection filter.

All but the Royco data were recorded on magnetic tape in the aircraft by means of a 42-channel magnetic tape data logger. The data tapes were returned to the Visibility Laboratory to be processed using the computer facilities at the University of California, San Diego.

A ground-based station near each flight track contained effectively duplicate instrumentation for obtaining optical data on all but the first of the four field trips. On all four trips a contrast reduction meter for measuring earth-to-space beam transmittance and path radiance was used by the ground team.

TABLE OF CONTENTS

LIST OF ILLUSTRATIONS

RELATED CONTRACTS AND PUBLICATIONS

Related Contracts: None

Publications:

Duntley, S. Q., R. W. Johnson, and J. I. Gordon, "Airborne Measurements of Optical Atmospheric Properties in Southern Germany," AFCRL-72-0255, SIO Ref. 72-64 (July 1972).

Duntley, S. Q., R. W. Johnson, and J. I. Gordon, "Airborne and Ground-Based Measurements of Optical Atmospheric Properties in Central New Mexico," AFCRL-72-0461, SIO Ref. 72-71 (September 1972).

Duntley, S. Q., R. W. Johnson, and J. I. Gordon, "Airborne Measurements of Optical Atmospheric Properties, Summary and Review," AFCRL-72-0593, SIO Ref. 72-82 (November 1972).

Duntley, S. Q., R. W. Johnson, and J. I. Gordon, "Airborne Measurements of Optical Atmospheric Properties in Southern Illinois," AFCRL-TR-73-0422, SIO Ref. 73-24 (July 1973).

Duntley, S. Q., R. W. Johnson, and J. I. Gordon, "Airborne and Ground-Based Measurements of Optical Atmospheric Properties in Southern Illinois," AFCRL-TR-74-0298, SIO Ref. 74-25 (June 1974).

Duntley, S. Q., R. W. Johnson, and J. I. Gordon, "Airborne Measurements of Optical Atmospheric Properties in Western Washington," AFCRL-TR-75-0414, SIO Ref. 75-24 (September 1975).

Gordon, J. I., J. L. Harris, Sr., and S. Q. Duntley, "Measuring Earth-to-Space Contrast Transmittance from Ground Stations," Appl. Opt. **12**, 1317–1324 (1973).

Gordon, J. I., C. F. Edgerton, and S. Q. Duntley, "Signal-Light Nomogram," J. Opt. Soc. Am. **65**, 111–118 (1975).

GLOSSARY AND NOTATION

The notation used in reports and journal articles produced by the Visibility Laboratory staff follow, in general, the rules set forth in pages 499 and 500, Duntley *et al* (1957). These rules are:

Each optical property is indicated by a basic (parent) symbol.

A presubscript may be used with the parent symbol as an identifier, e.g., b indicates background while t denotes an object.

A postsubscript may be used to indicate the length of a path of sight, e.g., r denotes an *apparent* property as measured at the end of a path of sight of length r, while o denotes an *inherent* property based on the hypothetical concept of a photometer located at zero distance from an object.

A postsuperscript*, or a postsubscript$_*$, is employed as a mnemonic symbol signifying that the radiometric quantity has been generated by the scattering of ambient light reaching the path from all directions.

The parenthetical attachments to the parent symbol denote altitude and direction. The letter z indicates altitude in general; z_t is used to specify the altitude of an object. The direction of a path of sight is specified by the zenith angle θ and the azimuth ϕ. In the case of irradiances, the downwelling irradiance is designated by d, the upwelling by u.

$A(z)$ Albedo at altitude z, defined by the equation $A(z) \equiv H(z,u)/H(z,d)$.

${}_sA(z)$ Scalar albedo at altitude z, defined by the equation ${}_sA(z) \equiv h(z,u)/h(z,d)$.

AGL Above ground level.

$C_o(z_t,\theta,\phi)$ Inherent universal contrast determined for a path of sight of zero length at altitude of the object z_t in the direction of zenith angle θ and azimuth ϕ. This property is defined by the equation

$$C_o(z_t,\theta,\phi) \equiv \frac{{}_tN_o(z_t,\theta,\phi) - {}_bN_o(z_t,\theta,\phi)}{{}_bN_o(z_t,\theta,\phi)} .$$

$C_r(z,\theta,\phi)$ Apparent universal contrast as determined at altitude z from the end of path of sight of length r in the direction of the zenith angle θ and azimuth ϕ. This property is defined by the equation

$$C_r(z,\theta,\phi) \equiv \frac{{}_tN_r(z,\theta,\phi) - {}_bN_r(z,\theta,\phi)}{{}_bN_r(z,\theta,\phi)} .$$

g Acceleration of gravity.

$H(z)$ Scale height at altitude z, the height of a homogeneous atmosphere having the density of the layer at altitude z.

$H(z,d)$ Irradiance produced by downwelling flux as determined on a horizontal flat plate at altitude z. In this report d is used in place of the minus sign in the notation $H(z_{t},-)$ which appears in Duntley (1969). This property may be defined by the equation

$$H(z,d) \equiv \int_{2\pi} N(z,\theta',\phi') \cos\theta' \, d\Omega .$$

$H(z,u)$ Irradiance produced by upwelling flux as determined on a horizontal flat plate at altitude z. Here u is substituted for the plus sign formerly used in the notation $H(z,+)$.

$h(z)$ Scalar irradiance. This may be defined as the radiant flux arriving at a point, from all directions about that point, at altitude z (Tyler and Preisendorfer, 1962):

$$h(z) \equiv h(z,d) + h(z,u) .$$

$h(z,d)$ Scalar irradiance produced by downwelling flux. This may be defined as the radiant flux from the upper hemisphere arriving at a point at altitude z.

${}_kh(z,d)$ Scalar irradiance defined as the radiant flux from the upper hemisphere sky (flux from the sun is not included) arriving at a point at altitude z.

${}_sh(z)$ Scalar irradiance defined as the radiant flux from the sun arriving at a point at altitude z.

$h(z,u)$ Scalar irradiance produced by upwelling flux. This may be defined as the radiant flux from the lower hemisphere arriving at a point at altitude z.

$L(z)$ Attenuation length at altitude z. This property is the reciprocal of the attenuation coefficient, that is,

$$L(z) \equiv \alpha(z)^{-1} .$$

$\bar{L}(z)$ Equivalent attenuation length is defined as

$$\bar{L}(z) = \frac{-z}{\ln T_z(0,0)} .$$

$m_\infty(z,\theta)/m_\infty(z,0)$ Relative optical airmass.

$N(z,\theta,\phi)$ Radiance as determined from altitude z in the direction specified by zenith angle θ and azimuth ϕ.

${}_bN_o(z_t,\theta,\phi)$ Inherent background radiance as determined at altitude of the photometer z_t at zenith angle θ and azimuth ϕ.

${}_bN_r(z,\theta,\phi)$ Apparent background radiance as determined at altitude z from the end of a path of sight of length r at zenith angle θ and azimuth ϕ. This property may be defined by the equation

$${}_bN_r(z,\theta,\phi) \equiv {}_bN_o(z_t,\theta,\phi)\, T_r(z,\theta) + N_r^*(z,\theta,\phi) .$$

${}_sN_\infty(0,\theta_s,0°)$ Apparent radiance of the center of the solar disk as determined at ground-level altitude from the end of path of sight of length ∞ from out of the atmosphere to ground at zenith angle of the sun θ_s.

${}_tN_o(z_t,\theta,\phi)$ Inherent radiance of an object as determined at altitude of the photometer z_t at zenith angle θ and azimuth ϕ.

${}_tN_r(z,\theta,\phi)$ Apparent radiance of an object as determined at altitude z from the end of a path of sight of length r at zenith angle θ and azimuth ϕ. This property may be defined by the equation

$${}_tN_r(z,\theta,\phi) \equiv {}_tN_o(z_t,\theta,\phi)\, T_r(z,\theta) + N_r^*(z,\theta,\phi) .$$

$N_q(z,\theta,\phi)$ Equilibrium radiance at altitude z with the direction of the path of sight specified by zenith angle θ and azimuth ϕ. This property is a point function of position and direction.

$\bar{N}_q(z,\theta,\phi)$ Effective equilibrium radiance for a path of sight from out of the atmosphere to altitude z in the direction specified by zenith angle θ and azimuth ϕ. This property may be defined by the equation

$$\bar{N}_q(z,\theta,\phi) \equiv N^*_\infty(z,\theta,\phi)/[1 - T_\infty(z,\theta)] \ .$$

This property may also be denoted as a function of angle from light source (sun or moon) β, i.e., $\bar{N}_q(z,\beta)$.

$N_*(z,\theta,\phi)$ Path function at altitude z with the direction of the path of sight specified by zenith angle θ and azimuth ϕ. This property is defined by the equation

$$N_*(z,\theta,\phi) \equiv \int_{4\pi} \sigma(z,\beta')\, N(z,\theta',\phi')\, d\Omega \ .$$

This property also is a point function of position and direction.

$N^*_r(z,\theta,\phi)$ Path radiance as determined at altitude z at the end of a path of sight of length r in the direction specified by zenith angle θ and azimuth ϕ.

$N^*_\infty(0,\gamma_s,180°)$ Sky radiance at a scattering angle of 90° from the sun. Also the path radiance for the path of sight of length ∞ from out of the atmosphere to ground-level altitude at a zenith angle equal to the solar elevation angle γ_s.

$n(z)$ Index of refraction at altitude z.

$P(z)$ Pressure at altitude z.

psia Pressure, absolute, pounds per square inch.

psid Pressure, differential, pounds per square inch.

${}_bR_o(z_t,\theta,\phi)$ Inherent background reflectance as determined at the altitude of an object z_t and viewed at zenith angle θ and azimuth ϕ.

$R_q(z,\theta,\phi)$ Equilibrium reflectance is defined as $R_q(z,\theta,\phi) \equiv N_q(z,\theta,\phi)\, \pi / H(z,d)$.

$R_r^*(z,\theta,\phi)$ Directional path reflectance as determined at altitude z at the end of a path of sight of length r in the direction specified by zenith angle θ and azimuth ϕ.

R/M(0) Universal gas constant.

$\overline{S_\lambda T_\lambda}$ Standardized relative spectral response of filter/cathode combination where S_λ is spectral sensitivity of the multiplier phototube cathode and T_λ is spectral transmittance of optical filter.

s(z) Total volume scattering coefficient as determined at altitude z. This property may be defined by the equation

$$s(z) \equiv \int_{4\pi} \sigma(z,\beta)\, d\Omega \ .$$

In the absence of atmospheric absorption, the total volume scattering coefficient is numerically equal to the attenuation coefficient.

${}_M s(z)$ Total volume scattering coefficient for Mie scattering at altitude z.

${}_R s(z)$ Total volume scattering coefficient for Rayleigh scattering at altitude z.

T(z) Temperature in degrees Kelvin at altitude z.

$T_r(z,\theta)$ Beam transmittance as determined at altitude z for a path of sight of length r at zenith angle θ. This property is independent of azimuth in atmospheres having horizontal uniformity. It is always the same for the designated path of sight or its reciprocal.

W_λ Spectral emittance (power/unit of area) of electromagnetic flux from a plane surface.

${}_c W_\lambda$ Spectral emittance of calibration source.

W'_λ Spectral emittance of anticipated field scene.

$\bar{y}$ Symbol for visual efficiency function.

ZSV Zero scale value. The zero point on the linear scale when the radiometric or photometric quantity x is equal to a reference radiometric or photometric quantity x_o as shown in the equation

$$\log[x_o/x] = 0 \ .$$

z Altitude, usually used as above ground level.

z_t — Altitude of an object.

$a(z)$ — Volume attenuation coefficient as determined at altitude z. In the absence of atmospheric absorption, the attenuation coefficient is numerically equal to the volume scattering coefficient.

β — Symbol for scattering angle of flux from a light source. It is equal to the angle between the line from the source to the observer and the path of sight.

β' — Symbol for scattering angle of flux from a discrete part of the sky. It is equal to the angle between the direction specified by θ' and ϕ' and the path of sight.

γ_s — Elevation angle of the sun. The solar elevation angle is the complement of the sun zenith angle, $\gamma_s = 90° - \theta_s$.

Δ — Symbol to indicate incremental quantity and used with r and z to indicate small, discrete increments in path length r and altitude z.

δ_λ — Response area is defined as $\delta_\lambda = \Sigma(\overline{S_\lambda T_\lambda})\,\Delta\lambda$.

ϵ_λ — Spectral emissivity of tungsten filament.

ζ — Symbol for radius of the earth in Eq. 2.13 and 2.15 and Figure 2-2.

θ — Symbol for zenith angle. This symbol is usually used as one of two coordinates to specify the direction of a path of sight.

θ' — Symbol for zenith angle usually used as one of two coordinates to specify the direction of a discrete portion of the sky.

λ — Symbol for wavelength.

$\bar{\lambda}$ — Mean wavelength is defined as $\bar{\lambda} \equiv \Sigma\lambda(\overline{S_\lambda T_\lambda})\,\Delta\lambda / \delta\lambda$.

$\rho(z)$ — Density at altitude z.

σ — Symbol for volume scattering function. Parenthetical symbols may be added; for example, β may be used to designate the scattering angle from a source. In Gordon (1969) the parenthetical symbols are z and β for altitude and scattering angle.

$\sigma(z,\beta)/s(z)$ — Proportional directional volume scattering function. This may be defined by the equation

$$\int_{4\pi} [\sigma(z,\beta) / s(z)] \equiv 1 .$$

$_{b}\tau_{r}(z,\theta,\phi)$ Contrast transmittance as determined at altitude z at the end of a path of sight of length r and specified by zenith angle θ and azimuth ϕ. This property is *not* independent of azimuth and is *not* the same for the designated path of sight and its reciprocal.

ϕ Symbol for azimuth. The azimuth is the angle in the horizontal plane of the observer between a fixed point and the path of sight. The fixed point may be, for example, true north, the bearing of the sun, or the bearing of the moon. This symbol is usually used as one of two coordinates to specify the direction of a path of sight.

ϕ' This symbol for azimuth is usually used as one of two coordinates to specify the direction of a discrete portion of the sky.

Ψ Angular solar radius at true earth-to-sun distance.

$\bar{\Psi}$ Angular solar radius at mean solar distance.

Ω Symbol for solid angle. For a hemisphere

$$\Omega = 2\pi \text{ steradians;}$$

for a sphere $\Omega = 4\pi$ steradians.

1. INTRODUCTION

This is the final report prepared under Contract F19628-73-C-0013. It discusses activities, accomplishments, and recommendations related to an atmospheric optical properties measurement program conducted during the interval 1 September 1972 through 30 June 1975. The experimental measurement flights made during this contract interval as part of the Visibility Laboratory's ongoing program of environmental documentation are identified in Table 1-1. Selected sets of the measurements from the project data bank have been presented in three preceding reports: AFCRL-54-73-0422, "Airborne Measurements of Optical Atmospheric Properties in Southern Illinois," Duntley, *et al.* (1973), AFCRL-TR-74-0298, "Airborne and Ground-Based Measurements of Optical Atmospheric Properties in Southern Illinois," Duntley, *et al.* (1974), and AFCRL-TR-75-0414, "Airborne Measurements of Optical Atmospheric Properties in Western Washington," Duntley, *et al.* (1975a). These measurements and the computations related to their use are examples of one facet of the Laboratory's continuing development of improved techniques for predicting, by calculation from physical data, the probabilities with which any object can be visually detected and recognized.

The radiometer spectral responses were standardized during this contract interval, as illustrated in Fig. 1-1. They were discussed in detail in Section 3.6 of AFCRL-TR-73-0422, Duntley, *et al.* (1973).

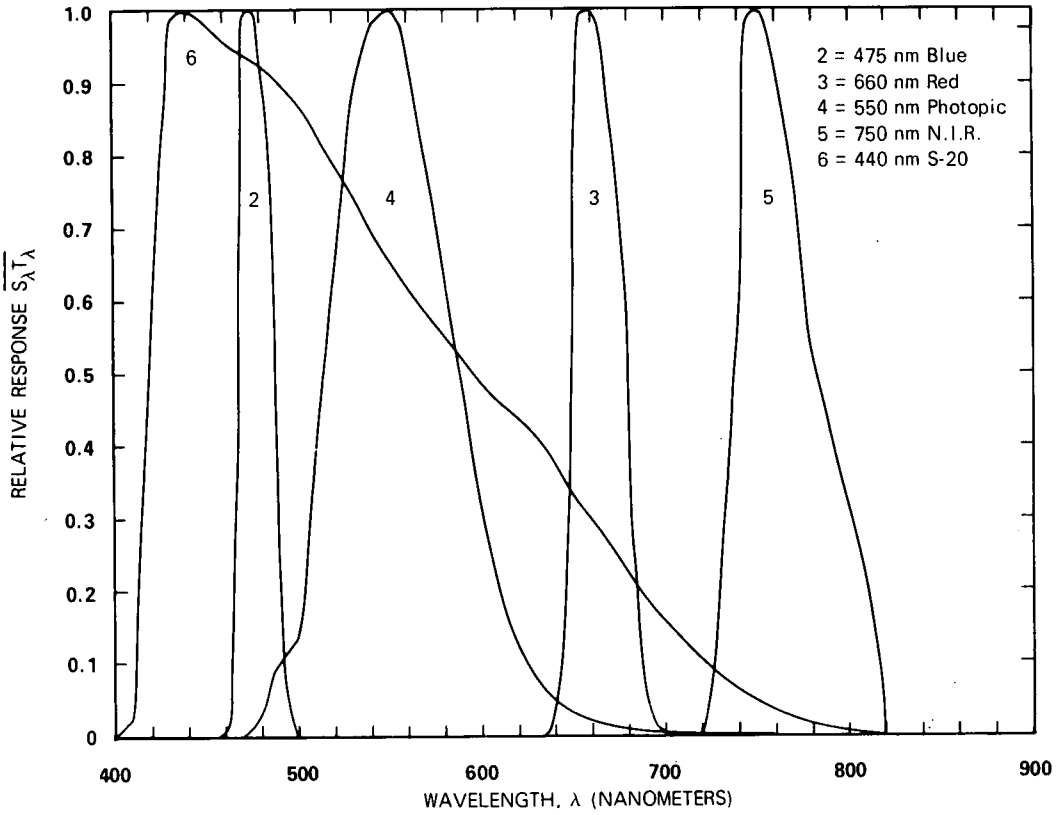

Fig. 1-1. Standard Spectral Responses.

Table 1-1

Summary of Airborne Data Collection Flights

Flight No.	Dates	Project Title*	Geographic Location
C-250 – C-256	13 Jan 73 to 31 Jan 73	GATEWAY	St. Louis, Missouri
C-270 – C-290	9 May 73 to 15 Jun 73	HAVEN VIEW II	Northern Germany
C-300 – C-310	17 Jan 74 to 12 Feb 74	SEMINOLE	Mexico Beach, Florida
C-350 – C-360	9 Jul 74 to 28 Jul 74	SEEKVAL	Rainier, Washington

* Project titles are for procedural identification only and are not necessarily utilized or recognized by agencies or organizations outside the Visibility Laboratory.

A summary of the methods used in the derivation of the reported optical atmospheric properties is presented in Section 2, as are the various modifications to the techniques which have been instituted during this contract interval.

The optical instrumentation, developed at the Visibility Laboratory, has been reported in detail in AFCRL-70-0137, Duntley, *et al.* (1970), AFCRL-72-0593, Duntley, *et al.* (1972c), and AFCRL-TR-73-0422, Duntley, *et al.* (1973). The portions of this instrumentation, installed in USAF C-130A SN50022, which generated the raw data upon which the reported properties are based consisted of an integrating nephelometer for determining the total and proportional directional scattering coefficients and two sky scanning radiometers for recording upper and lower hemisphere radiances. A ground-based integrating nephelometer similar to the airborne instrument provided the ground-level value of the total volume scattering coefficient. Major revisions to the hardware have occurred at several intervals during the life of this current contract. They are summarized and discussed in Section 3.

Data collection methods throughout this report interval have remained similar to those described in AFCRL-TR-73-0422, Duntley, *et al.* (1973), with one procedural variation to shorten elapsed data times. A short review of the technique is discussed in Section 4.

The computer techniques used during this report interval are also well-documented in the previously identified references. A summary of the most significant alterations introduced during this contract is presented in Section 5.

Section 6 presents a review of the field trips and a summary of existing data bank and its status.

A discussion of projected procedural updates and recommendations for future program activities is included in Section 7.

2. THEORY

2.1 AIRBORNE DATA DERIVATIONS

The three scientific reports from this contract period, Duntley, *et al.* (1973, 1974, and 1975), contain the optical properties of various downward-inclined paths of sight based on daytime atmospheric optical measurements. These properties include natural irradiance upon horizontal plane surfaces, scalar irradiance, total volume scattering coefficient, atmospheric beam transmittance, path radiance, directional path reflectance, and directional terrain reflectance.

GENERAL APPROACH

The Visibility Laboratory maintains a continuing program of improving the techniques for predicting, by calculation from physical data, the probabilities with which any object can be visually detected and recognized. The program is multifaceted in that it involves the development of techniques and expertise in several different technical areas, each related to the visual detection and recognition task. Several of the major areas are, for example, measurement and analysis of typical terrain characteristics and scene reflectances, studies in the restoration of atmospherically distorted images, measurement and analysis of the optical properties of the atmosphere, studies into the perceptual capabilities of the human visual system and its electro-optical counterparts. The joint application of the techniques perfected in each of these specialty areas, results in the final determination of detection probabilities. Inclusion of allowances for *a priori* information and reasoning processes by the brain enable the probabilities of recognition, classification, and identification of real world objects to be predicted.

The instrumental and computational organization for pursuing the improvement of techniques related to documenting the optical properties of the atmosphere is summarized in Figures 2-1, 2-2, and 2-3. These three figures illustrate the experimental inter-relationships between the various pieces of project hardware, listed in rectangles at the top of each figure and discussed in Section 3, the radiometric measurements made by them, and the subsequent computational chains associated with each of the measured values. The optical properties, listed in the blocks at or near the bottom of each figure, are derived in accordance with the theoretical considerations discussed in Section 2, Duntley, *et al.* (1973). Through an examination of these generalized flow charts, one can readily evaluate this portion of the program's flexibility and self-checking redundancies. The capability to generate equivalent optical properties from separate independent data sources, as indicated within these three figures, is the key feature in ensuring advancements in technical expertise and data quality.

MODIFICATIONS COMPLETED

Previous reports from this experimental project described the initial techniques used in the derivation of the optical properties illustrated in Fig. 2-1, 2-2, and 2;3. Two reports from the previous contract interval, Duntley, *et al.* (1972a and b), discussed the derivation of typical daytime optical properties, and one report, Duntley, *et al.* (1972c), summarized the procedural modifications as of August 1972.

More recently, additional improvements to the computational methods have been instituted and discussed in Duntley, *et al.* (1973, 1974, and 1975a). Among these early modifications to the computational techniques, one which has now become fully implemented is the separation of the sun radiance from the remainder of the upper hemisphere radiances. This separation has materially improved the computational results for several derived quantities, including downwelling irradiance, path function, and equilibrium radiance. The form for computing equilibrium radiance, for example, may now be given by

$$N_q(z,\theta,\phi) = {}_sN_r(z,\theta_s,0^\circ)\frac{\sigma(z,\beta)}{s(z)}\,d\Omega_s + \int_{4\pi} N(z,\theta',\phi')\,\frac{\sigma(z,\beta')}{s(z)}\,d\Omega \quad . \tag{2.1}$$

In the first term of Eq. 2.1, ${}_sN_r(z,\theta,0^\circ)$ is the apparent sun radiance and in the second, $N(z,\theta',\phi')$ represents the apparent radiance of the remainder of the sky and underlying terrain. In most computations, however, the sun scalar irradiance ${}_sh(z)$ is used in lieu of the equivalent form ${}_sN_r(z,\theta_s,0^\circ)\,d\Omega_s$.

This report, Duntley, *et al.* (1975b), summarizes the most significant of those improvements developed and implemented during the 1972–1975 contract interval.

Since one of the sources of variability in the data for a given flight is the change in sun zenith angle over the flight interval, a programming option was added which allows the use of an average sun zenith angle per filter or per flight in the computations of path radiance and irradiance. An option was also added to allow external specification of the space-to-highest-flight-altitude beam transmittance. This was originally designed to be used for cloudy days with an estimated beam transmittance. However, it can also be used to insert the value of beam transmittance obtained by ratioing the space-to-earth transmittance measured by the contrast reduction meter and the high-altitude-to-earth transmittance from the nephelometer data, as suggested in Section 8 of Duntley, *et al.* (1972b).

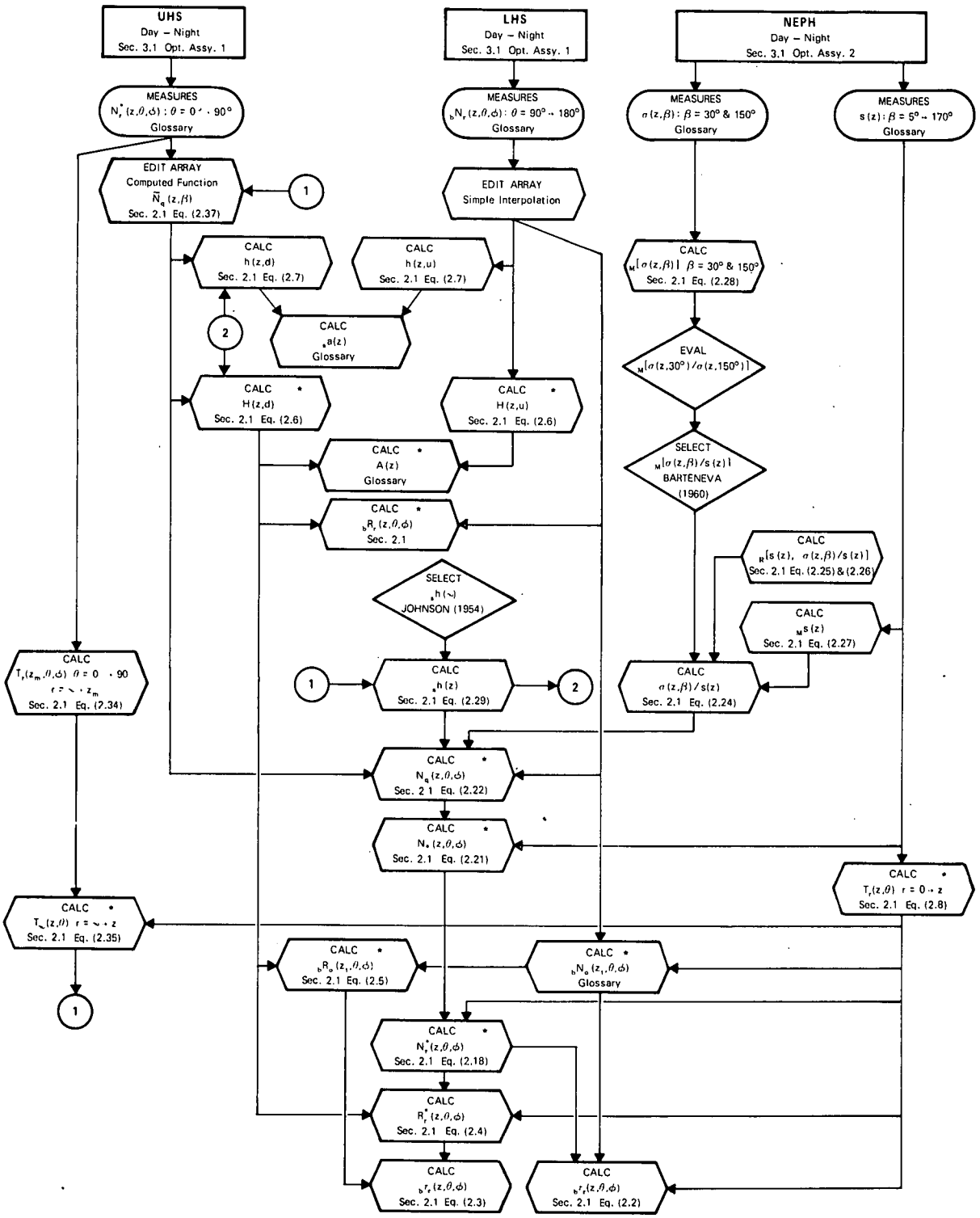

★ Indicates existence of validation measurement in backup data set.

* Section and Equation Numbers refer to Duntley, *et al.* (1973).

Fig. 2-1. Computations from Basic Airborne Data.

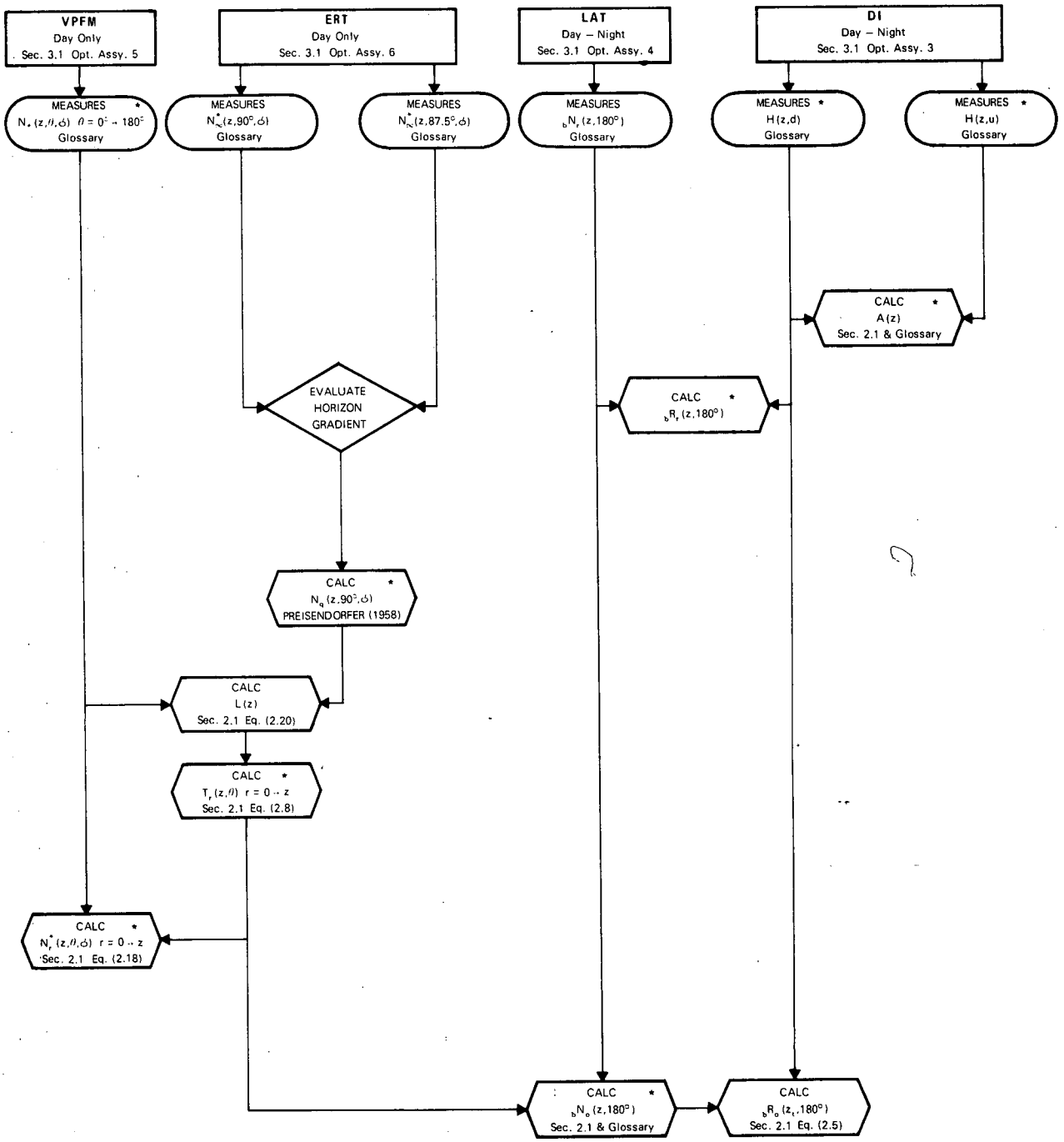

★ Indicates utilization as direct validation of computed values.

* Section and Equation Numbers refer to Duntley, *et al.* (1973).

Fig. 2-2. Computations from Backup Airborne Data.

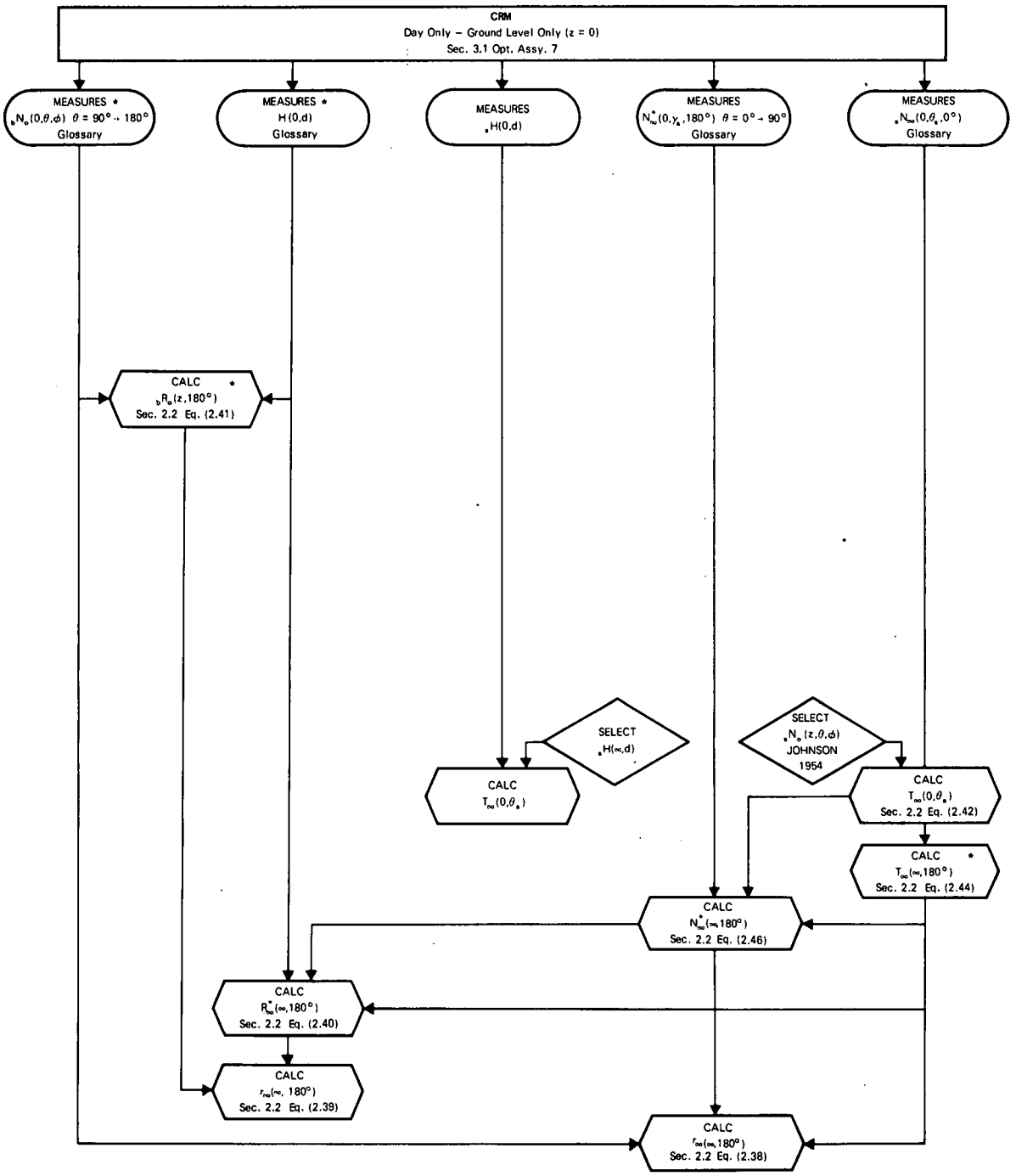

★ Indicates utilization as direct validation of computed values.

* Section and Equation Numbers refer to Duntley, *et al.* (1973).

Fig. 2-3. Computations from Specialized Ground Data.

Another modification was to compute the space-to-altitude transmittance from sky radiance ratios. When the sky at the highest flight altitude is clear of clouds, the transmittance due to scattering from out of the atmosphere to the highest flight altitude is computed from the ratio of the sky radiances $N^*_\infty(z,\theta,\phi)/N^*_\infty(z,\theta',\phi')$ at equivalent scattering angles from the sun (AFCRL-TR-73-0422, Duntley, *et al.* (1973), Eq. 2.34):

$$\frac{N^*_\infty(z,\theta,\phi)}{N^*_\infty(z,\theta',\phi')} = \frac{\left[1 - T_\infty(z,0^\circ)^{m_\infty(z,\theta)/m_\infty(z,0^\circ)}\right]}{\left[1 - T_\infty(z,0^\circ)^{m_\infty(z,\theta')/m_\infty(z,0^\circ)}\right]} . \qquad (2.2)$$

Equation 2.2 is solved for vertical transmittance $T_\infty(z,0^\circ)$ by using an iterative technique. Then a series of sky radiance measurements is used to obtain an average transmittance in order to minimize the effect of the precision error of the sky radiances.

Continued concern about adequate specification of the sky and sun radiances has led to a number of recent modifications to measuring and computational techniques. These modifications apply only to the third scientific report from this contract period, AFCRL-TR-75-0414, Duntley, *et al.* (1975a).

One instrument modification allowed for the addition of a separate sun mode scanner interval to the measurement pattern. This modification is described in detail in Section 4.1 of AFCRL-72-0593, Duntley, *et al.* (1972c). Subsequent to the modification, all abnormalities in the upper hemisphere data array attributable to slow phototube decay have disappeared. Extensive compensatory software adjustments to the data array are no longer required, and the resultant data quality is excellent.

A second instrument modification which influenced our computational procedures was further development of the variable path function meter. This was particularly fortunate since attenuation coefficient could thus be recovered from the measured path function values and computed values of equilibrium radiance in the event that nephelometer data were unavailable. When the nephelometer optical system became optically contaminated during five of the eight flights reported in AFCRL-TR-75-0414, Duntley, *et al.* (1975a), this procedure, described in Section 8 of that report, was fortuitously implemented.

A nomogram for prediction of the sighting range for white, steady-burning signal lights is contained in an article begun prior to but submitted and published during this contract interval: Gordon, *et al.* (1975). The nomogram may be used for slant-path sightings by applying values of equivalent attenuation length as a function of altitude. The optical properties presented in each of the scientific reports during this contract interval, AFCRL-TR-73-0422, AFCRL-TR-74-0298, AFCRL-TR-75-0414, Duntley, *et al.* (1973, 1974, and 1975a) and the previous contract interval, AFCRL-72-0255, AFCRL-72-0461, Duntley, *et al.*, (1972a and 1972b), have all contained graphs of equivalent attenuation length as a function of altitude based on the atmospheric measurements of total scattering coefficient.

MODIFICATIONS IN PROCESS

Upward Path of Sight. The optical properties of various upward-inclined paths of sight are derivable

from the same daytime atmospheric optical measurements employed for the downward paths of sight. The basic differences are as follows: The upward path of sight is defined for zenith angles θ between 0 and 90 degrees, the sensor at ground level, and the object at altitude z_t above ground level. The path reflectance $R_r^*(0,\theta,\phi)$ becomes a function of the upwelling irradiance $H(z_t,u)$ at the object altitude, as well as the path radiance $N_r^*(0,\theta,\phi)$ and the beam transmittance $T_r(0,\theta,\phi)$:

$$R_r^*(0,\theta,\phi) = \pi N_r^*(0,\theta,\phi)/[H(z_t,u)\, T_r(0,\theta,\phi)] \ . \tag{2.3}$$

The average background reflectance ${}_bR_o(z_t,\theta,\phi)$ becomes a function of the sky radiance $N_\infty^*(z_t,\theta,\phi)$ and the upwelling irradiance:

$${}_bR_o(z_t,\theta,\phi) = \pi N_\infty^*(z_t,\theta,\phi)/H(z_t,u) \ . \tag{2.4}$$

For paths of sight from 85 to 90 degrees in zenith angle the incremental path length Δr for the incremental altitude Δz = 30 meters (98.4 feet) is significantly shorter at 6 kilometers (the typical highest flight altitude) than it is at ground level due to the curvature of the earth. Therefore, for these paths of sight, the incremental path length Δr_i is computed from

$$\Delta r_i = \left\{1 - \left[\frac{n(0)}{n(z_i)}\ \frac{\zeta}{(\zeta + z_i)}\ \sin\theta\right]^2\right\}^{-\frac{1}{2}} \Delta z \ , \tag{2.5}$$

where ζ is the radius of the earth and $n(z)$ is the refractive index. The square of the refractive index ratio is computed from a form given by Kasten (1965) as

$$\left[\frac{n(0)}{n(z_i)}\right]^2 = 1 + 2[n(0) - 1]\left[1 - \frac{\rho(z_i)}{\rho(0)}\right] \ . \tag{2.6}$$

The computer program for calculating the path radiance and path reflectance from the airborne atmospheric optical measurements is currently being modified so that the paths of sight may be defined as either upward or downward inclined.

Proportional Directional Scattering Function. We are continuing the attempt to recover the proportional directional scattering function $\sigma(z,\beta)/s(z)$ from sky radiances. The equation being used is Eq. 23 from Gordon (1969):

$$\sigma(z,\beta)/\,s(z) = \left[\bar{N}_q(z,\theta,\phi) - \frac{{}_k h(z,d) + h(z,u)}{4\pi}\right] \div \left[{}_s h(\infty)\, T_\infty(z,\theta_s)\right] \quad . \tag{2.7}$$

where $\bar{N}_q(z,\theta,\phi)$ is the average effective equilibrium radiance derived from the sky radiances and the space-to-altitude beam transmittance $T_\infty(z,\theta)$, ${}_k h(z,d)$ is the scalar irradiance from the sky, $h(z,u)$ is the upwelling scalar irradiance, and ${}_s h(\infty)$ is the inherent sun irradiance.

If enough effective equilibrium radiances are available for a broad coverage of angles from the sun, i.e., as $\beta = 0 \rightarrow 180°$, the proportional scattering function resulting from Eq. 2.7 may be integrated, and the result should equal 1:

$$\int_{4\pi} \frac{\sigma(z,\beta)\, d\Omega}{s(z)} = 1 \quad . \tag{2.8}$$

Another check on the consistency of the data is to integrate the effective equilibrium radiance to obtain the total scalar irradiance [Eq. 22 from Gordon (1969)]:

$$h(z) = \int_{4\pi} \bar{N}_q(z,\theta,\phi)\, d\Omega \quad . \tag{2.9}$$

This value may then be compared to the total scalar irradiance based upon the integration of the sky and terrain radiances $N(z,\theta,\phi)$ and the scalar sun irradiance:

$$h(z) = {}_s h(z) + \int_{4\pi} N(z,\theta,\phi)\, d\Omega \quad . \tag{2.10}$$

The results to date of the attempts at scattering function recovery are inconsistent, thus indicating the need for further development of the method before the results can be used with confidence.

2.2 GROUND-BASED DATA DERIVATIONS

The first scientific report of this contract period, AFCRL-TR-73-0422, Duntley, *et al.* (1973), contained no ground-based data. The second report, AFCRL-54-74-0298, Duntley, *et al.* (1974), presented the available ground-based data on irradiance, terrain reflectance, and total and directional scattering coefficients which were measured at Scott Air Force Base, a site remote from the flight tracks reported in AFCRL-TR-73-0422 and AFCRL-TR-74-0298, Duntley, *et al.* (1973 and 1974). The third scientific report,

AFCRL-54-75-0414, Duntley, *et al.* (1975a), made use of a few selected ground-based measurements since the ground-based data site was directly beneath the flight track.

The derivation and validation of the basic method of measuring earth-to-space path radiance and beam transmittance from ground stations is contained in an article prepared during the previous contract interval but submitted and published during the current contract interval: Gordon, *et al.* (1973). There is a large body of in-house data being processed by this method with various broad band filters in the visible part of the spectrum. The first sizeable portion of that data taken by portable instruments during the 1962 to 1967 period to obtain downwelling irradiance, sky irradiance, vertical earth-to-space beam transmittance, path radiance, and path reflectance has been converted into metric units, stored on magnetic tape for easy access, and summarized in an in-house technical note. This catalog of data has proven useful in evaluating current contrast reduction meter measurements. The photopic measurements from this period will be described later in this section.

DIAGNOSTIC DEVELOPMENTS COMPLETED

Optical Properties of Photopic Rayleigh Atmosphere. To aid in the evaluation of the ground-based measurements of optical properties of the atmosphere it is useful to develop limiting values. An upper limit in clarity is a day with only Rayleigh scattering. A computer program was developed to produce a set of values for the photopic Rayleigh atmosphere using the atmospheric optical model developed earlier in Gordon (1969). The pertinent equations and assumptions used to compute these Rayleigh values are summarized in the following paragraphs.

For each path of sight in the lighted atmosphere there is an equilibrium radiance that is transmitted unchanged because the loss (attenuation of image-forming light) is exactly counterbalanced by the gain due to the scattering of sunlight and skylight toward the sensor. In this model, the equilibrium radiance for ground level is expressed as a function of the proportional directional scattering function $\sigma(0,\beta)/s(0)$, the space-to-ground beam transmittance $T_\infty(0,0°)$, and the scalar albedo ${}_sA$ [Eq. 41 of Gordon (1969)]:

$$N_q(0,\beta) = {}_sh(0)\left\{\frac{\sigma(0,\beta)}{s(0)} + \frac{{}_sA}{4\pi} + \frac{\left(\frac{1+{}_sA}{4\pi}\right)\int_{2\pi}\left[\frac{\sigma(0,\beta')}{s(0)} + \frac{{}_sA}{4\pi}\right][1 - T_\infty(0,\theta')]\,d\Omega}{1 - \left(\frac{1+{}_sA}{4\pi}\right)\int_{2\pi}[1 - T_\infty(0,\theta')]\,d\Omega}\right\}. \quad (2.11)$$

The ${}_sh(0)$ is the sun scalar irradiance at ground level, and β is the scattering angle from the sun.

The proportional directional scattering function $\sigma(\beta)/s$ for Rayleigh scattering is not a function of altitude so the parenthetical modifier for altitude is not used. It is found by

$$\sigma(\beta)/s = 3(1 + f\cos^2\beta)/[4\pi(3 + f)] \ , \tag{2.12}$$

where f is the polarization defect factor. This factor is a function of the ratio of the weak to strong polarized component at $\beta = 90$ degrees for pure air; a ratio of 0.04 results in a factor of 0.923 [Tousey and Hulburt (1947)]. The effect of the defect factor on $\sigma(\beta)/s$ is equal to or less than ± 2 percent which for our purposes can be considered negligible. Therefore $f = 1$ was used in the computations.

The sun scalar irradiance is found by using Eq. 27 from Gordon (1969):

$$_sh(0) = {}_sh(\infty)\, T_\infty(0,\theta_s) \ , \tag{2.13}$$

where $_sh(\infty)$ is the scalar solar irradiance out of the atmosphere of the earth and θ_s is the zenith angle of the sun.

The beam transmittance at a zenith angle θ is obtained from the vertical beam transmittance and the relative airmass $m_\infty(0,\theta)/m_\infty(0,0°)$:

$$T_\infty(0,\theta) = T_\infty(0,0°)^{m_\infty(0,\theta)/m_\infty(0,0°)} \ . \tag{2.14}$$

Relative airmass values are from Kasten (1965).

The ground-level sky radiance is the path radiance from space to ground $N^*_\infty(0,\theta,\phi)$. The sky radiance is a function of the equilibrium radiance and the beam transmittance of the path [Eq. 11, Gordon (1969)]:

$$N^*_\infty(0,\theta,\phi) = N_q(0,\beta)\ [1 - T_\infty(0,\theta)] \ . \tag{2.15}$$

The scattering angle β is a function of the path of sight zenith angle θ and azimuth ϕ and the sun zenith angle θ_s:

$$\cos\beta = \sin\theta_s \sin\theta \cos\phi + \cos\theta_s \cos\theta \ . \tag{2.16}$$

The total downwelling irradiance on a fully exposed horizontal surface H(0,d) is composed of the sun irradiance $_sH(0,d)$ and the sky irradiance $_kH(0,d)$:

$$H(0,d) = {}_sH(0,d) + {}_kH(0,d) \ . \tag{2.17}$$

The sun irradiance is the scalar irradiance times the cosine of the zenith angle of the sun:

$$_sH(0,d) = {}_sh(0)\cos\theta_s \ . \tag{2.18}$$

The sky irradiance is the integral of the sky radiances weighted by the cosine of the sky radiance zenith angle:

$$ {}_{k}H(0,d) = \int_{2\pi} N^{*}_{\infty}(0,\theta,\phi) \cos\theta \, d\Omega \ . \tag{2.19} $$

The vertical earth-to-space path radiance is obtained by rewriting Eq. 2.15 for the appropriate path of sight:

$$ N^{*}_{\infty}(\infty,180°,0°) = N_{q}(0,\beta)\,[\,1 - T_{\infty}(\infty,180°)\,] \ . \tag{2.20} $$

The first assumption of the model presented in Gordon (1969) is that the point function equilibrium radiance for a given path of sight does not change with altitude, thus simplifying the requirement for satisfying Eq. 2.20.

The scattering angle for the vertical path of sight is a direct function of the sun zenith angle:

$$ \beta = 180° - \theta_{s} \ . \tag{2.21} $$

For vertically downward paths of sight, predictions of the vertical path radiance require sky radiance measurements in directions having equivalent scattering angles. Under conditions of small sun zenith angles, there are no directions appropriate for these measurements. For these cases an approximation of the sky radiance at $\beta = 90°$ is used. Therefore, for comparison to these measured values of path radiance, a second set of path radiances were derived for the vertical path of sight using the equilibrium radiance at $\beta = 90°$.

By definition, the earth-to-space vertical path reflectance is a function of the previously defined path radiance, beam transmittance, and downwelling irradiance [Eq. 4 of Duntley (1969)]:

$$ R^{*}_{\infty}(\infty,180°,0°) = \pi\, N^{*}_{\infty}(\infty,180°,0°) / [\,H(0,d)\, T_{\infty}(\infty,180°)\,] \ . \tag{2.22} $$

Comparison of Gordon Model to Other Models. Sky radiances or luminances have been computed for the photopic Rayleigh atmosphere by Coulson, *et al.* (1960), Pyaskovskaya-Fesenkova (1957), and Tousey and Hulburt (1947). To facilitate comparison of the Gordon (1969) model to these other models, computations were made with the Gordon model using the same vertical beam transmittance, solar irradiance out of the atmosphere, solar zenith angles, and albedo as for the other models.

Coulson, *et al.* (1960) gave a table of downward radiation emerging from the bottom of the atmosphere (or sky radiance) for a Rayleigh atmosphere of optical thickness 0.15 (equivalent to vertical-space-to-earth beam transmittance of 0.861) and a μ_o of 0.80 ($\mu_o = \cos\theta_s$), therefore the sun zenith angle is 36.8 degrees). They use a sun scalar irradiance at ground level of π, therefore the sun scalar irradiance out of the atmosphere is $\pi/T_\infty(0,\theta_s) = 3.79$ [$T_\infty(0,36.8°) = 0.829$ when the vertical transmittance is 0.861]. They use albedos of 0, 0.25, and 0.80. The same values were assumed for scalar albedo in the Gordon-model computations. The sky radiance values for the two models for azimuths toward and away from the sun are graphed in Fig. 2-4. The comparison is best nearest the horizon in both azimuths. The values for the Gordon model near the zenith are slightly higher than for the Coulson model.

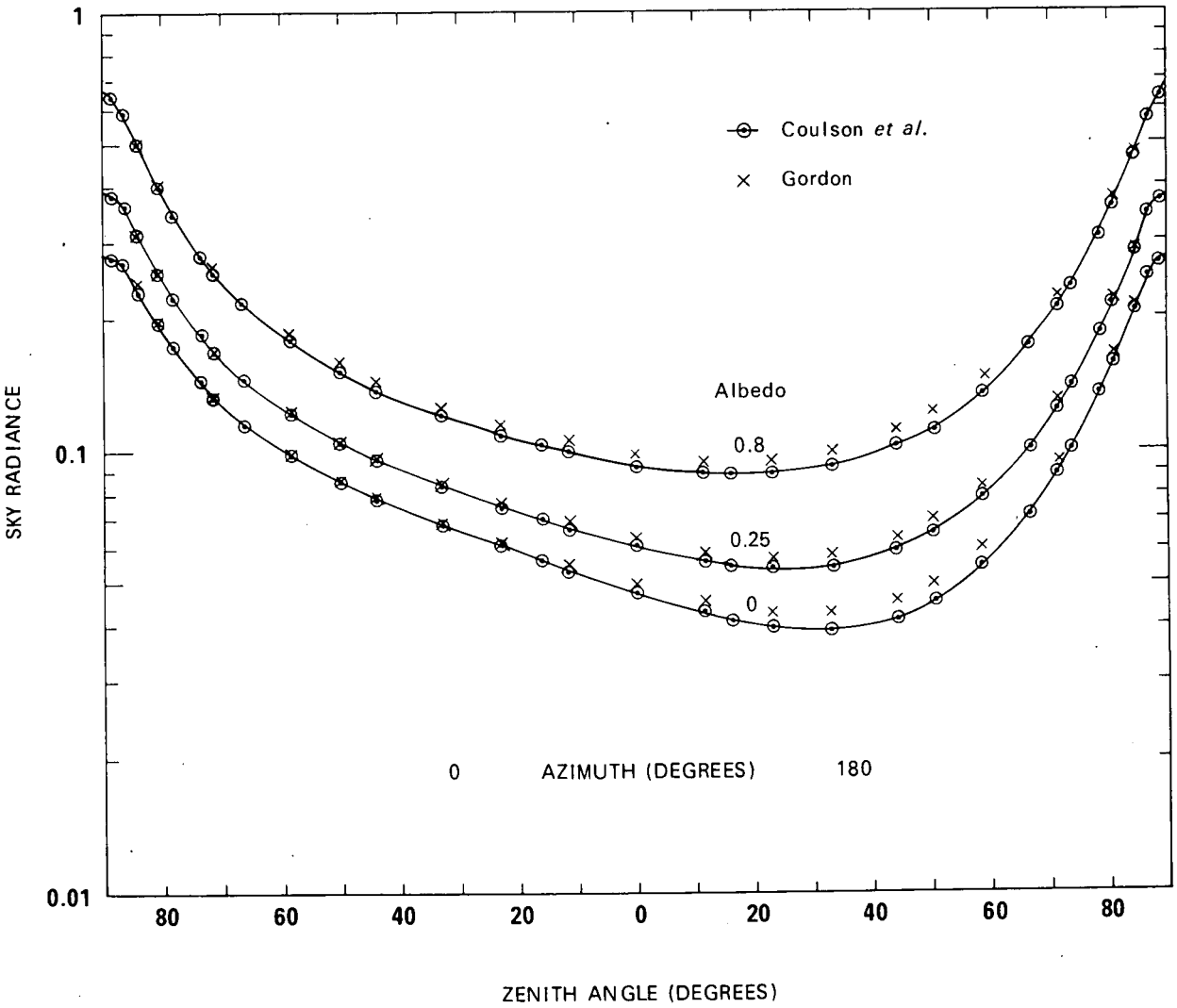

Fig. 2-4. Rayleigh Sky Radiance for Coulson, *et al.* and Gordon Using a Vertical Beam Transmittance of 0.861, Sun Zenith Angle of 36.8°, and a Sun Scalar Irradiance at Ground Level of π.

Since the Gordon model always has a flatter curve of sky radiance versus zenith angle than the Coulson model, the question arises as to whether the assumption of a curved earth as used by the Gordon equations versus a flat earth as assumed by Coulson, *et al.* would account for this kind of a difference. Therefore, the values were recalculated substituting $\sec\theta$ for airmass in all the equations for the Gordon model. Using $\sec\theta$ instead of airmass increased the Gordon values less than 1 percent at the zenith, about 2.5 percent at 80 degrees, and about 4 percent at 84.3 degrees. These differences are scarcely large enough even at the large zenith angles to be critical and are, in fact, barely discernable on the graph.

Pyaskovskaya-Fesenkova (1957) presents an isoluminance plot showing the results of calculations for a Rayleigh atmosphere with a vertical space-to-earth beam transmittance of 0.861, a solar zenith angle of 60 degrees, and a sun illuminance out of the atmosphere of 13 stilbs or lu/cm^2. It was indicated that the equations used were from V. V. Sobolev and that they were appropriate for albedos other than zero, although the albedo was not specified. The computations for the Gordon model were made using scalar albedos of 0.10 and 0.25. These are depicted as continuous curves in Fig. 2-5. The angular positions of the isoluminance values for the Pyaskovskaya-Fesenkova graph were estimated and are depicted in Fig. 2-5 as separate points. This accounts for the slight irregularity of these points. The curve for 0.25 albedo is close to the Pyaskovskaya-Fesenkova values near the horizon but higher near the zenith.

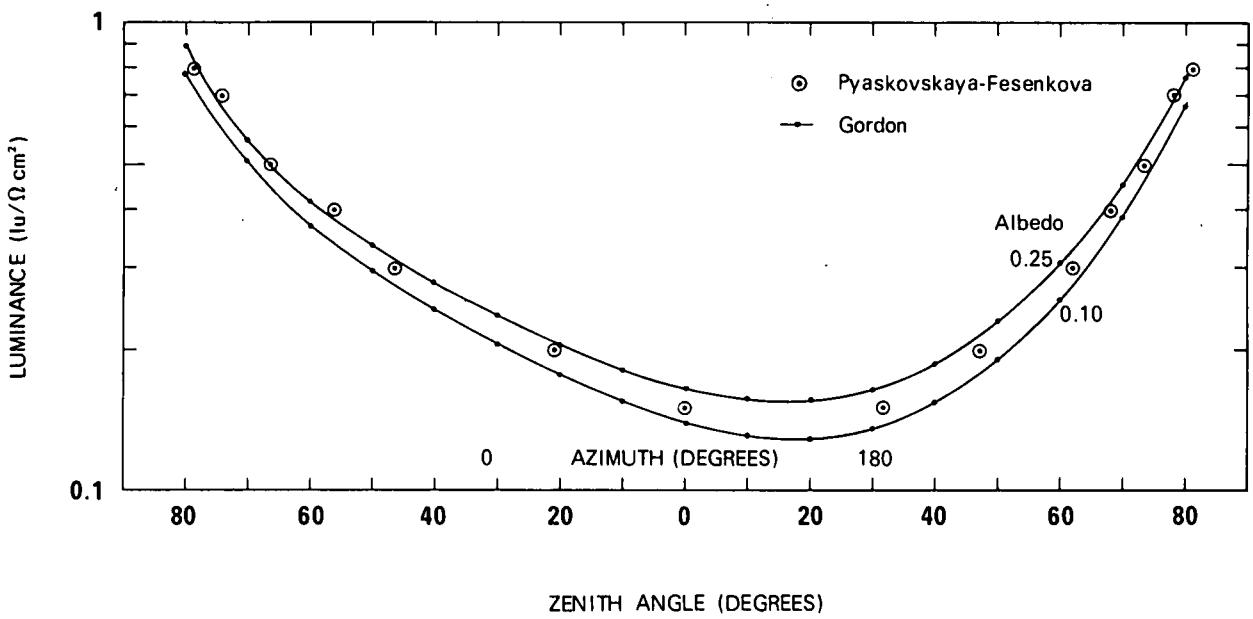

Fig. 2-5. Rayleigh Sky Luminances (lu/cm^2 or stilbs) for Pyaskovskaya-Fesenkova and Gordon Using Vertical Earth-to-Space Beam Transmittance of 0.861, a Sun Illuminance Out of the Atmosphere of 13 lu/cm^2, and a Sun Zenith Angle of 60 Degrees.

Tousey and Hulburt (1947) computed sky luminance at a 10 000-foot (3.05-kilometer) altitude, assuming a Rayleigh scattering function, a diffuse reflectivity of the earth of 0.20, an illuminance of the sun out of the atmosphere of 13600 lu/ft^2, and a ground-level scattering coefficient of 0.016 km^{-1}. The equivalent vertical thicknesses of the atmosphere, reduced to kilometers of air at normal temperature and pressure, were based on the U.S. Standard Atmosphere (1962) and were 8 kilometers for 0 altitude and 5.50 kilometers for a 10 000-foot altitude. The optical thickness due to ozone at the top of the atmosphere was 0.023 (a transmittance of 0.977).

In order to compare the sky values of the Gordon model to those of Tousey and Hulburt, a calculation of ground-level equilibrium luminance was made in which the scalar albedo was assumed equivalent to the diffuse reflectance 0.20. The transmittance in the Gordon model is due to scattering only, therefore the vertical beam transmittance from out of the atmosphere to ground level used in Eq. 2.11 was $T_\infty(0,0°) = \exp - [8(0.017)] = 0.873$. Since Tousey and Hulburt decrease the sun illuminance by assuming ozone absorption at the top of the atmosphere, the sun illuminance ${}_sh(0)$ was computed from Eq. 2.13 using the vertical beam transmittance from out of the atmosphere to ground level as $T_\infty(0,0°) = \exp -[8(0.017 + 0.23] = 0.853$. The calculation was made for the largest and smallest solar zenith angle reported by them, 75 degrees and 0 degrees. The sky luminances at the 10 000-foot altitude were then computed using an equation similar to Eq. 2.15,

$$N^*_\infty(z,\theta,\phi) = N_q(z,\beta)\,[1 - T_\infty(z,\theta)] \quad , \tag{2.23}$$

where z = 10 000 ft. (3.05 kilometers), $N_q(z,\beta) = N_q(0,\beta)$, and $T_\infty(z,0°) = \exp[-5.5(0.017)] = 0.911$. The resultant sky values are graphed in Fig. 2-6. The solid lines represent the values given by Tousey and Hulburt (1947), Table I. These are the same values as those given in Table 1 of Hulburt (1957). The values for the Gordon model compare well near the zenith and are slightly lower near the horizon for the sun at a zenith angle of 75 degrees. For the 0-degree sun zenith angle, the Gordon values are consistently a little higher than the Tousey and Hulburt values, comparing best at the zenith.

In conclusion, the photopic Rayleigh sky radiance values from the Gordon model compare reasonably well to the values of Coulson, *et al.* (1960), Pyaskovskaya-Fesenkova (1957), and Tousey and Hulburt (1947).

Comparison of Rayleigh Values to Visibility Laboratory Data from 1962 to 1967. For comparison to various Visibility Laboratory ground-based measurements, calculations for the Gordon model were made using a photopic scalar sun irradiance out of the atmosphere of 1.89E3* w/m$^2\mu$m based upon the spectral sun values of Johnson (1954) and a photopic Rayleigh space-to-sea-level beam transmittance $T_\infty(0,0°)$ of 0.907. The beam transmittance is based on the sea-level scale height and temperature for the U.S. Standard Atmosphere (1962) which is appropriate for 45 degrees latitude. The Rayleigh beam transmittance through the atmosphere does not change with sea-level temperature.

The ground-based earth-to-space contrast transmittance data measured between 1962 and 1967 with portable instruments contain 359 photopic observations. These observations were taken in conjunction with a number of field tests at 11 locations. The photopic earth-to-space vertical beam transmittances for

* The form 1.89E3 is an alternate format for 1.89 x 10^3, and is used throughout this report.

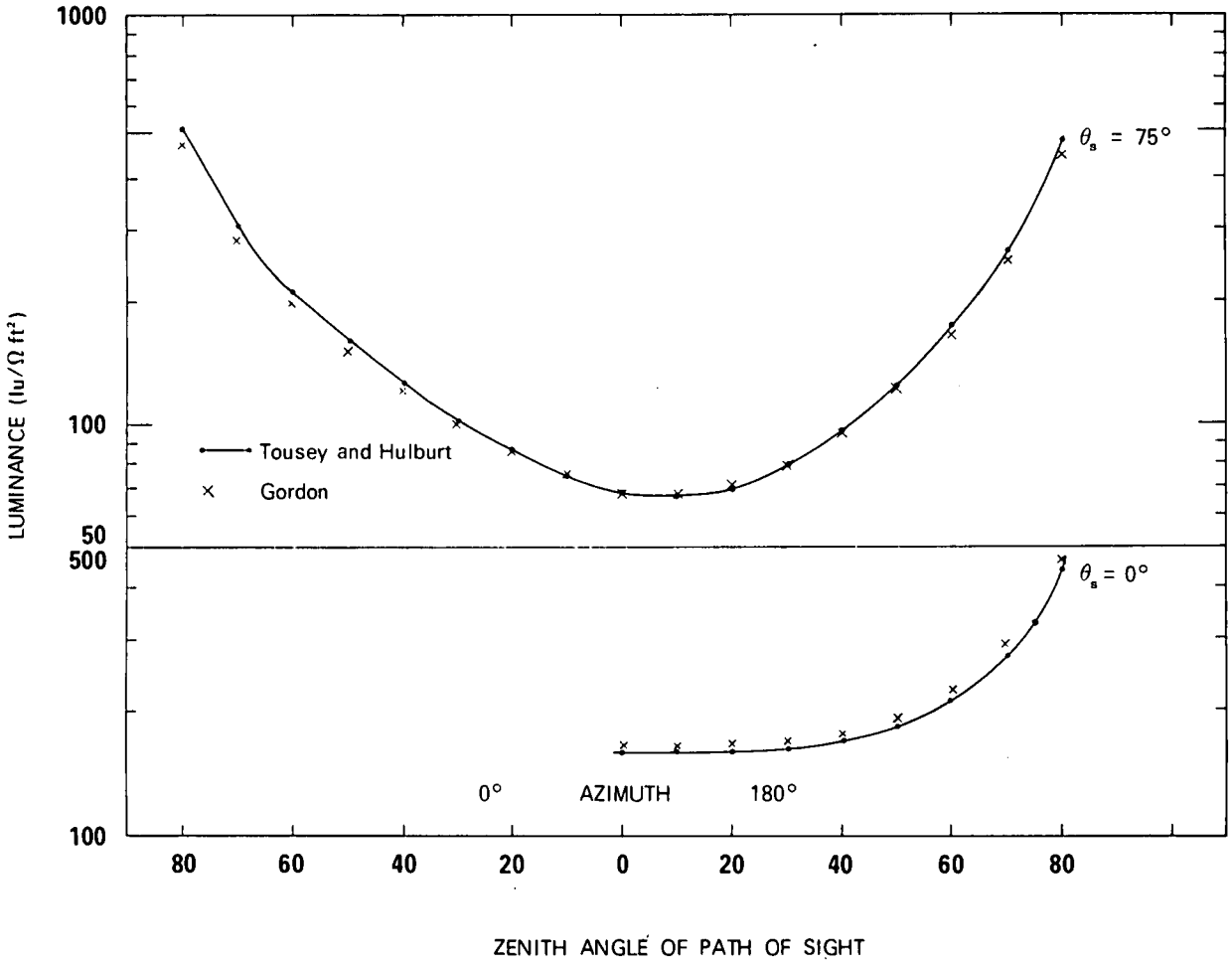

Fig. 2-6. Rayleigh Sky Luminance (lu/ft^2 at 10 000 feet) for Tousey and Hulburt (1947) and Gordon (1969) for Sun Illuminance Out of the Atmosphere of 13 600 lu/ft^2, Ground-Level Scattering Coefficient of 0.017 km^{-1}, and an Albedo of 0.20.

these data are graphed as a function of sun zenith angle in Fig. 2-7. The photopic data for this period is labeled as Filter 3. The symbols indicate the location or field experiment for each data point. The beam transmittance is computed from measurements of apparent radiance of the center of the sun, except for the Naval Ordnance Test Station (NOTS) data where shadow-intensity meter measurements were used instead. The average transmittance was 0.72 which is close to the value of 0.7 commonly used as the average clear-day photopic transmittance. The solid reference line is the Rayleigh photopic vertical earth-to-space transmittance.

The location labels indicate the following locations, field experiments, instruments, and number of photopic observations: NOTS was a field test at Naval Ordnance Test Station, China Lake, California during the summer of 1962; irradiometer and shadow-intensity meter data (103 observations) were taken in

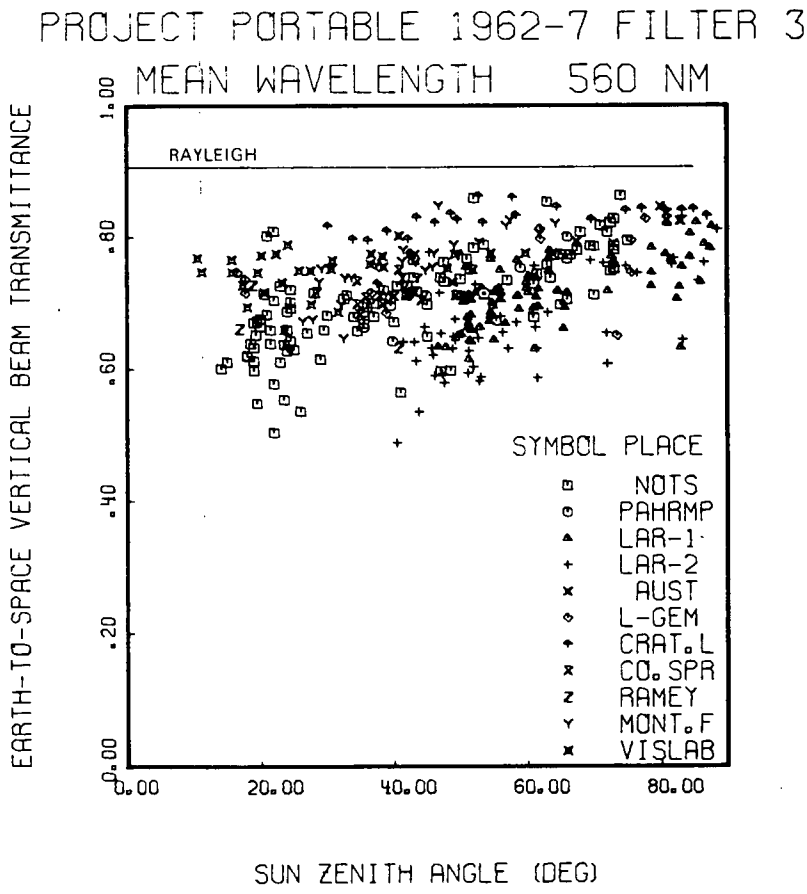

Fig. 2-7. Photopic Earth-to-Space Vertical Beam Transmittance as Measured by Visibility Laboratory Portable Instruments from 1962 to 1967.

conjunction with a field test [Gordon (1963)] involving airborne visual sightings at low altitude. PAHRMP was at Pahrump, Nevada, during the fall of 1963 and spring of 1964; solar transmissometer, irradiometer, and sky scanner data (7 observations) were measured in conjunction with a field test to validate the method of predicting earth-to-space contrast transmittance from ground stations [Duntley, *et al.* (1964) and Gordon, *et al.* (1973)]. LAR-1, LAR-2, AUST, and L-GEM were related to the space-to-earth visual acuity experiments conducted during Gemini flights V and VII, December 1964 through August 1965 [Duntley, *et al.* (1966) and Duntley, *et al.* (1968)]. The contrast reduction meter was used at all four sites. LAR-1 (81 observations) and LAR-2 (49 observations) were near Laredo, Texas, prior to the Gemini flights. AUST (8 observations) at Carnarvon, Australia, and L-GEM (12 observations) near Laredo, Texas, took place during the Gemini flights. CRAT. L, CO. SPR, and RAMEY were contrast reduction meter measurements made in August and September 1966 in conjunction with flights of the instrumented Air Force C-130 aircraft. CRAT. L (23 observations) was at Crater Lake, Oregon, and some of the airborne optical data have been reported by Boileau (1968a and b). CO. SPR (14 observations) was near Colorado Springs, Colorado; the related airborne data are published in Boileau (1968c). RAMEY (4 observations) was near Ramey Air Force

Base, Puerto Rico. MONT. F and VISLAB were contrast reduction meter measurements made during a study to determine the relationship between meteorological and optical properties of the atmosphere [Edgerton (1967)]. MONT. F (23 observations) was at Montgomery Field, San Diego, California, February through April 1967. VISLAB (29 observations) took place on the rooftop of a Visibility Laboratory building at San Diego, California, April to June 1967.

Downwelling irradiance H(0,d) is graphed in Fig. 2-8 as a function of sun zenith angle. The portable instrument data for 1962 to 1967 are designated by symbols indicating the beam transmittance in 0.10-transmittance increments; e.g., the symbol ⊙ indicates a transmittance of 0.85 ± 0.05 or values of transmittance from 0.80 to 0.899. These downwelling irradiances are all measured by an irradiometer. The two curves superimposed on the graph are the photopic Rayleigh atmosphere values for 1.0 albedo and the average clear-day values of Brown (1952).

The total downwelling irradiance for the photopic Rayleigh atmosphere with a scalar albedo of 1.0 should be an upper limit irradiance for clear skies with no clouds. The presence of scattered clouds, however, could conceivably raise the total irradiance due to high reflectance from the clouds when the sun is unobscured. The measured values of downwelling irradiance for the 1962 to 1967 period cluster about the average values of Brown and lie beneath the upper limiting values for the Rayleigh atmosphere.

The photopic sky irradiance ${}_{k}H(0,d)$ is graphed in Fig. 2-9 as a function of sun zenith angle. The portable instrument values for 1962 to 1967 are designated by symbols indicating the beam transmittance within ± 0.05. The curve superimposed on the graph represents the photopic Rayleigh atmosphere with a scalar albedo of zero.

The sky irradiance for the photopic Rayleigh atmosphere with a scalar albedo of zero may be a lower limit irradiance for clear skies with no clouds. Although most of the sky irradiance values lie above the Rayleigh curve, some 27 of the 353 values lie below. Of these, all but 4 were indicated as obtained during zero cloud cover. The values which are less than the Rayleigh values were obtained during three projects: NOTS, LAR-2, and VISLAB. The latter two projects, which had 18 of the questionable values, obtained sky irradiance by subtracting the calculated sun irradiance (based on measured beam transmittance) from the measured total downwelling irradiance. For these calculated values, the sky irradiance error is the difference between the total irradiance error and the transmittance error after both errors have been multiplied by factors greater than one. Therefore, a negative error in the total irradiance and a positive error in the beam transmittance will produce a large negative sky irradiance error which is more than the sum of the first two errors. Hence it is probably more reasonable to question these low values than the Rayleigh curve as a lower limit.

Of the remaining 9 low sky irradiance values, which were obtained at NOTS, all are only very slightly lower than the Rayleigh curve. These sky irradiance values were obtained with a shadow-intensity meter. The sky irradiance was measured when a metal bail shadowed the irradiometer from the sun. The measured value was then increased by a factor to attempt to correct for the portion of the sky occulted by the bail (which included most of the aureole around the sun). The bail was relatively large angularly so that these sky irradiance values are still a bit crude although a much more direct measure than the values obtained by subtraction.

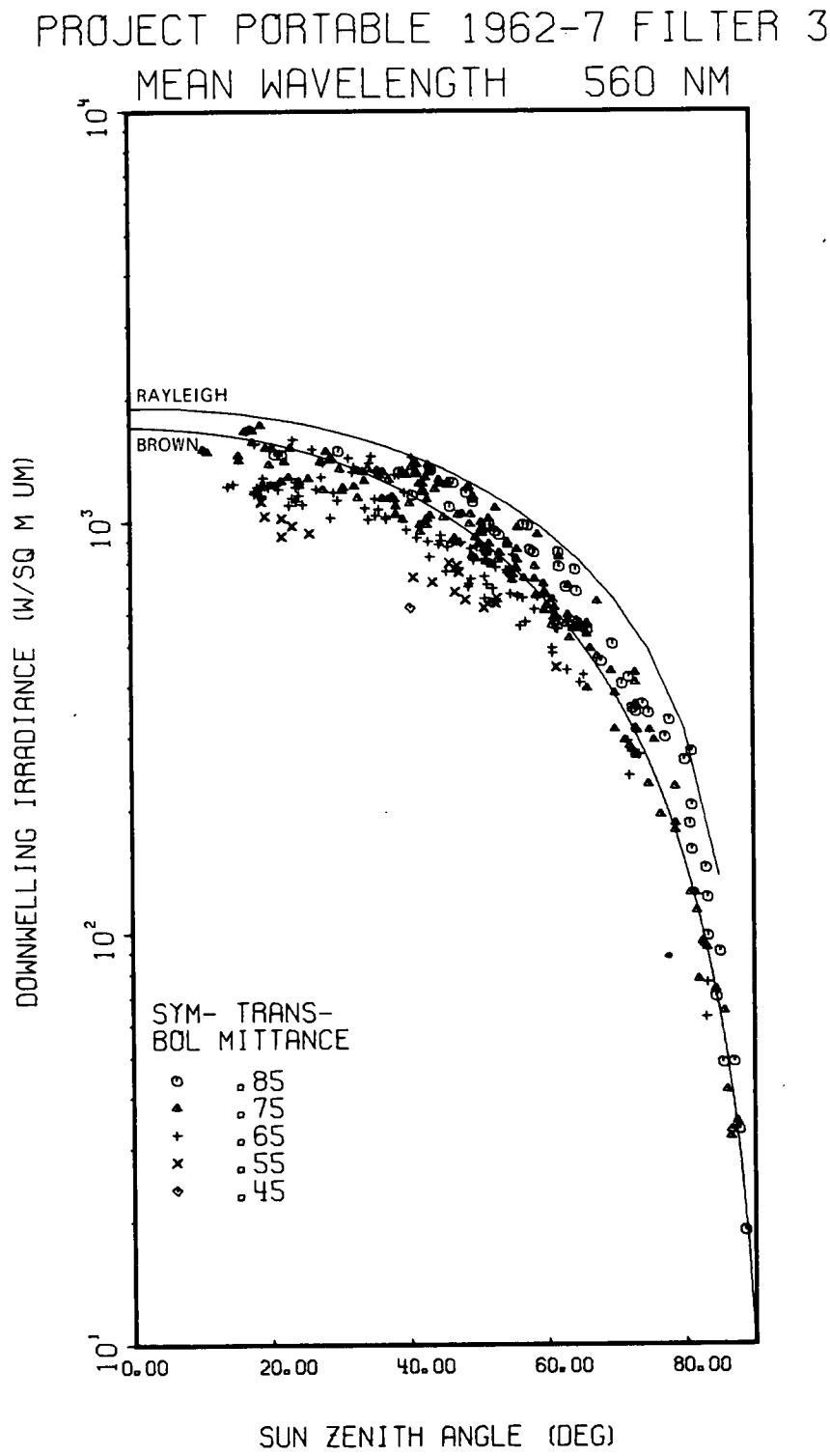

Fig. 2-8. Photopic Downwelling Irradiances as Measured by Visibility Laboratory Portable Instruments from 1962 to 1967 and Compared to the Photopic Rayleigh Atmosphere Values for a Scalar Albedo of 1.0 and from Brown (1952).

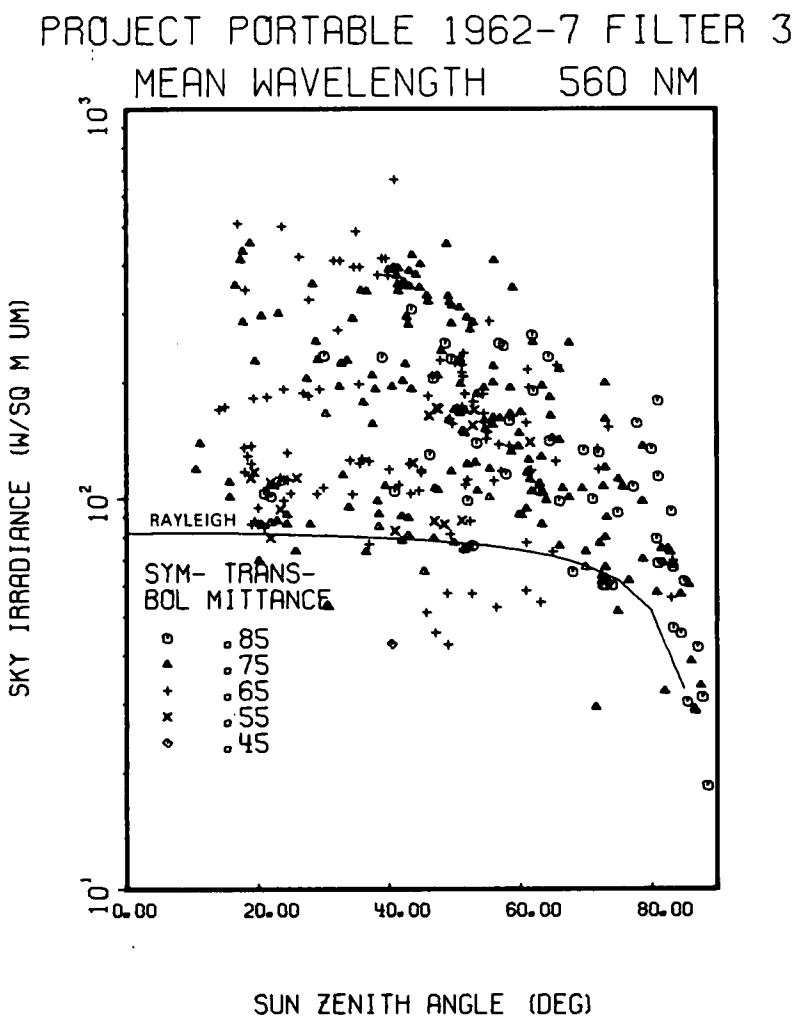

Fig. 2-9. Photopic Sky Irradiance as Measured by Visibility Laboratory Portable Instruments from 1962 to 1967 and Compared to the Photopic Rayleigh Atmosphere Values for a Scalar Albedo of Zero.

All things considered, the photopic Rayleigh curve for zero scalar albedo may be a reasonable lower limit for clear-sky irradiances. The values obtained which are below this limit should be used with great caution.

The photopic vertical path radiance from ground to space is graphed in Fig. 2-10 as a function of sun zenith angle. The portable instrument values for 1962 to 1967 are designated by symbols indicating the beam transmittance within ± 0.05. These path radiances are computed from the beam transmittance and the sky radiance at the same angle from the sun as the downward path of sight except for small sun zenith angles where the sky at 90 degrees from the sun is used. The curve superimposed on the graph represents the photopic Rayleigh atmosphere with a scalar albedo of zero for a scattering angle β of 90 degrees from the sun.

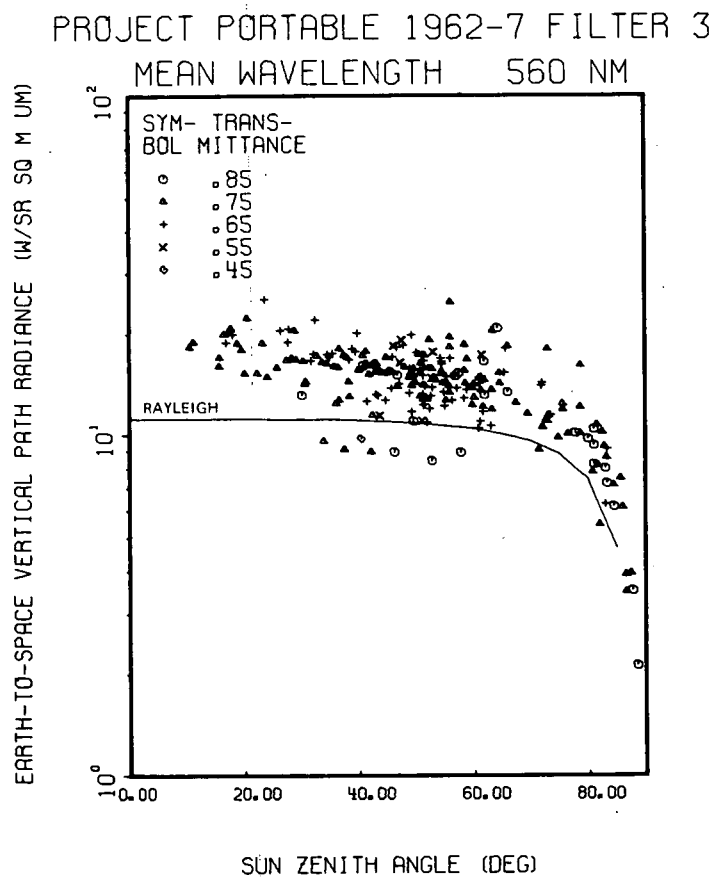

Fig. 2-10. Photopic Vertical Earth-to-Space Path Radiance as Measured by Visibility Laboratory Portable Instruments from 1962 to 1967 and Compared to the Photopic Rayleigh Atmosphere Values for $\beta = 90°$ for a Scalar Albedo of Zero.

The vertical earth-to-space path radiance for $\beta = 90°$ for the photopic Rayleigh atmosphere with a scalar albedo of zero may be a lower limit for the ground-based measurements of vertical sea-level-to-space path radiance for clear skies with no clouds. Nine of the measured path radiance values lie below this curve. Six of these values were measured at Crater Lake, Oregon, where ground level is at 2073 meters so the curve for sea-level altitude does not apply. The three remaining values were measured near Laredo, Texas, at a ground-level altitude of 152 meters but at the same time and date as three of the sky irradiances values which were below the Rayleigh sky irradiance curve. These three low values of path radiance should probably be regarded as questionable, as were the low sky irradiances.

The photopic vertical earth-to-space path reflectance is graphed in Fig. 2-11 as a function of sun zenith angle. The portable instrument values for 1962 to 1967 are designated by symbols indicating the vertical beam transmittance within ± 0.05. These path reflectances are computed from the beam transmittance, path radiance, and downwelling irradiance. The curve superimposed on the graph represents the photopic Rayleigh atmosphere with a scalar albedo of zero for a scattering angle β of 90 degrees from the sun.

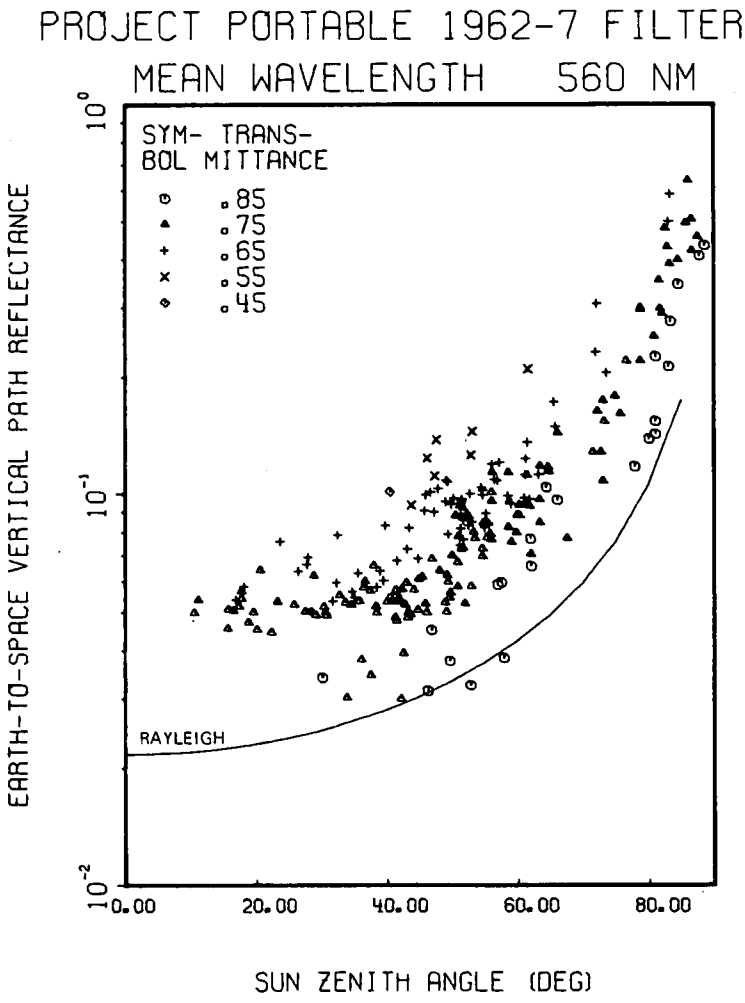

Fig. 2-11. Photopic Vertical Earth-to-Space Path Reflectance as Measured by Visibility Laboratory Portable Instruments from 1962 to 1967 and Compared to the Photopic Rayleigh Atmosphere Values for $\beta = 90°$ for a Scalar Albedo of Zero.

The vertical sea-level-to-space path reflectance for $\beta = 90°$ for the photopic Rayleigh atmosphere with a scalar albedo of zero should be a lower limit for the ground-based measurements of vertical path reflectance for clear skies with no clouds. Only two of the 1962 to 1967 values lie below the superimposed Rayleigh curve. Both of these values were measured at Crater Lake, Oregon, at a 2073-meter altitude, and therefore the Rayleigh curve which is for sea level does not apply.

In conclusion, based on comparison of the Rayleigh values to the ground-based Visibility Laboratory data for 1962 to 1967: The Rayleigh 1.0 albedo values for downwelling irradiance appear to be a reasonable upper limit. The Rayleigh zero albedo values for path reflectance appear to provide a reasonable lower limit. The Rayleigh zero albedo values for sky irradiance and path reflectance may be lower limits, but this is less certain.

DIAGNOSTIC DEVELOPMENTS IN PROCESS

Optical Properties of Non-Rayleigh Atmospheres Using the Gordon Model. In order to utilize the model atmosphere equations from Gordon (1969), it is necessary to specify a proportional directional scattering function and a vertical space-to-earth beam transmittance. Barteneva (1960) provides an extensive catalog of ground-level proportional directional scattering functions and an appropriate range of values of the ground-level volume scattering coefficient for each directional scattering function. By making some limiting assumptions about the structure of the scattering coefficient with altitude, it is possible to establish a range of appropriate vertical space-to-earth beam transmittance values for each directional scattering function. Model atmosphere computations using these sets of values for scattering function and transmittance enable us to explore the influence on given variables of a range of scattering functions for a constant transmittance, or a range of transmittances for one scattering function, and, finally, the overall range of reasonable values. Initial computations indicate this to be a fruitful approach. The results compare reasonably to the 1962 to 1967 data, and interesting relationships between variables are becoming evident.

Development of CRM-Type Data Catalog. There is available a second large body of ground-based data on the optical properties of the atmosphere appropriate for computing downwelling irradiance, earth-to-space beam transmittance, path radiance, and path reflectance. This second body of data consists of measurements made between January and September 1964 with automatic instruments mounted on the rooftop of one of the buildings at the Visibility Laboratory in San Diego. The instruments were a beam transmissometer, a sky scanning photometer, and an irradiometer. There are 937 data packages, about one-quarter of which were taken with a photopic filter. The rest are radiometric, limited to light in the visible spectrum: two relatively narrow band filters, with mean wavelengths of 459 and 661 nanometers, and a broad band filter with a mean wavelength of 505 nanometers. These data are for days with an unobscured sun and for a large range of solar zenith angles. The data have been converted into metric units, the derived optical properties computed, and initial data analysis begun. The data appear to be of excellent quality and worthy of report.

3. INSTRUMENTATION

The scientific instrumentation utilized during the interval 1 September 1972 through 30 June 1975 was first described in AFCRL 70-0137, Duntley, *et al.* (1970). In that report, the descriptions of the radiometric systems reflected the nighttime, low flux configuration for which they were initially designed and fabricated. Subsequent to that report, several additional reports were issued which described in general the basic system modifications required to convert the radiometric devices from nighttime to daytime operating configurations, and to debug the electrical and optical characteristics of the resultant modified system. The first was AFCRL-72-0255, Duntley, *et al.* (1972a), a second was AFCRL-72-0461, Duntley, *et al.* (1972b), and a third, AFCRL-72-0593, Duntley, *et al.* (1972c), which summarized all modifications up to August 1972.

The atmospheric visibility program at the Visibility Laboratory is planned and organized as a continuing program, and thus a variety of instrumentation modifications have been implemented subsequent to the period reported in AFCRL-72-0593, Duntley, *et al.* (1972c). The following paragraphs summarize the most significant of these recent improvements.

All primary instrument systems and subassemblies utilized during this report interval are tabulated in Table 3-1 and illustrated in their deployment configurations in Fig. 3-1 and 3-2.

Table 3-1. Project Instrumentation

I. Radiometric

- A. Multiplier Phototube Assembly
- B. Temperature Control Housing Assembly
- C. Optical Filter Assembly
- D. Radiometer Measuring Circuit Assembly
- E. Optical Collector Assembly
  1. Automatic 2π Scanner Assembly
  2. Integrating Nephelometer Mode Selector Head Subassembly
  3. Dual Irradiometer Assembly
  4. Large Aperture Telescope Assembly
  5. Variable Path Function Meter Assembly
  6. Equilibrium Radiance Telephotometer
  7. Contrast Reduction Meter

II. Meteorological

- A. Royco Model 220 Particle Counter
- B. Cambridge Model 137-C3 Aircraft Hygrometer System
- C. AN/AMQ-17 Aerograph Set
- D. Bourns Model 430/530 Absolute Pressure Transducer
- E. Bourns Model 509 Differential Pressure Transducer
- F. Bendix Model 566 Aspirated Hygrometer
- G. Science Associates Windspeed and Direction Set
- H. Taylor Model SMT-5-51 Aneroid Barometer

III. Control and Communication

- A. Automatic 2π Scanner Control Console
- B. Photometer Temperature Control Panel
- C. Optical Filter Control Panel
- D. Ten Slide Photometer Module
- E. Camera Control Panel
- F. Flight Dynamics Display Panel
- G. 42 Channel Data Logger
- H. 20 Channel Data Logger

IV. Photographic

- A. Automax G-1 Airborne Camera System
- B. Ground-Based Soligor System

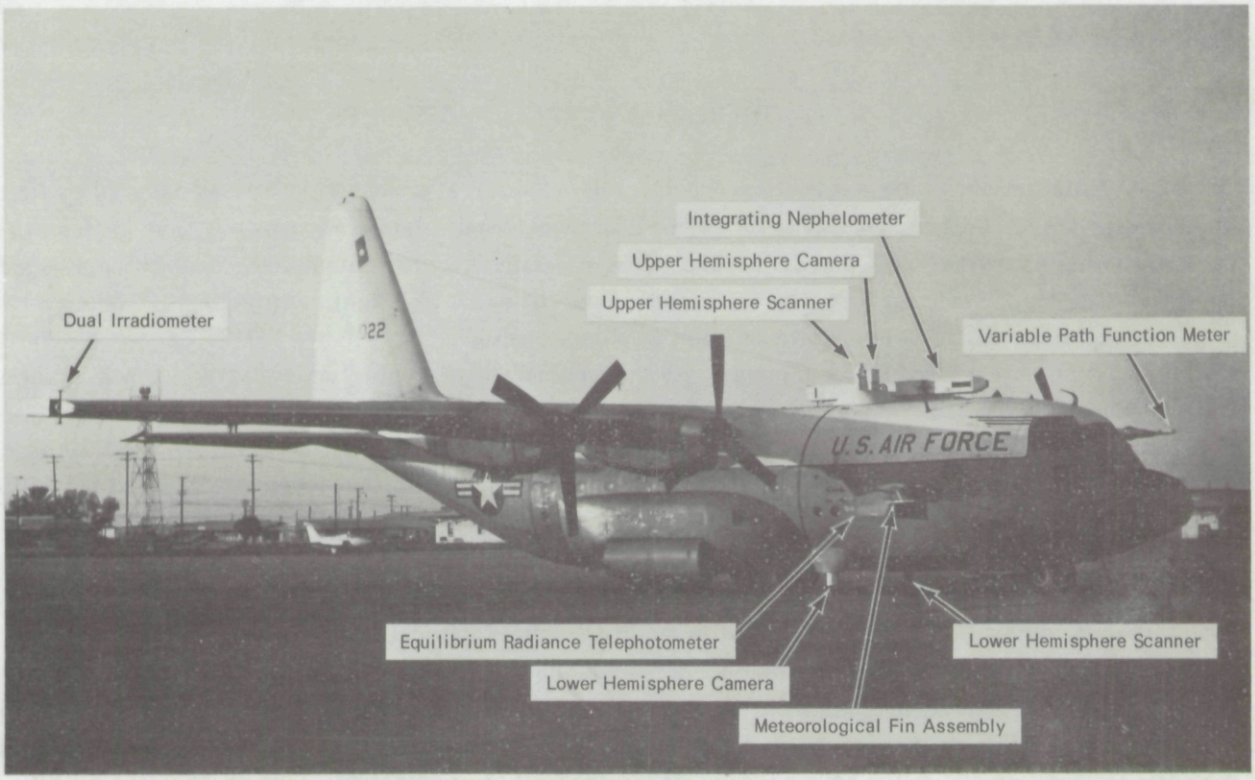

Fig. 3-1. C-130 Airborne Instrument System.

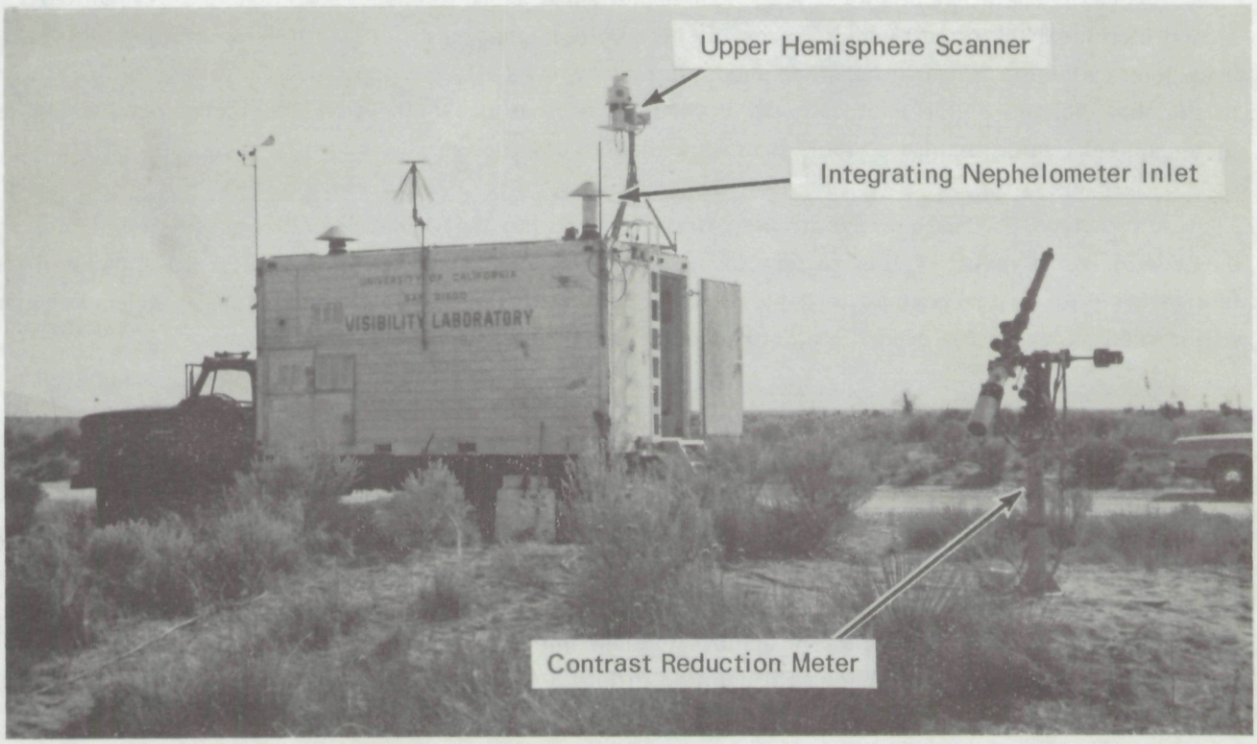

Fig. 3-2. Ground-Based Instrument System.

3.1 RADIOMETRIC SYSTEMS

MULTIPLIER PHOTOTUBE AND RADIOMETER MEASURING CIRCUIT ASSEMBLIES

The multiplier phototube assemblies and the related radiometer measuring circuit assemblies first described in AFCRL-70-0137, Duntley, *et al.* (1970), are no longer reliable systems and have been superceded during this contract interval. During the 1973–1974 interval, intermittent component failures began appearing with increasing regularity, as did system instabilities during flight. Retrofitting the photometer power supply slide with new externally mounted auxiliary supplies between the SEMINOLE and SEEKVAL deployments did not compensate for the gradually increasing rate of system unreliability. Since several key components in the model 5 photometer circuit were custom-built items, their replacement was prohibitively expensive in terms of both cost and delivery times. In order to resolve these system shortcomings, an entirely new integrated photometer (radiation detection) system was developed during the 1974–1975 interval.

The new integrated system is illustrated in Fig. 3-3 and 3-5. Several design features incorporated in this new package make it particularly well-suited to airborne applications. Since it is a highly compact, self-contained package, there is no longer any requirement to transmit high voltages from one part of the aircraft to another. The high voltage now is generated at the transducer location within the transducer housing. Additionally, the small size of the electronics package allows it to be contained within the same temperature controlled housing (Fig. 3-4) as the multiplier phototube, thus contributing even further to system stabilities.

The basic operation of this new system is the same as its predecessor. That is, it is basically a closed loop feedback circuit which servos the high voltage applied to the multiplier phototube. The feedback loop maintains a nearly constant anode current by inversely varying the high voltage with respect to the flux incident at the photocathode. Beyond its obvious packaging advantages, the new system is faster, quieter, safer, and more stable than its well worn predecessor.

A prototype of this new system was first flown during the deployment to western Washington in July, 1974. As a result of this satisfactorily completed field test, additional units are scheduled for fabrication prior to the next major deployment. A retrofit of the new system to each project radiometer will markedly improve the overall project capability and reliability.

TEMPERATURE CONTROL HOUSING ASSEMBLY

The temperature control housing utilized for the new integrated photometer system is slightly longer than the assembly illustrated in AFCRL-70-137, Duntley, *et al.* (1970). It is a retrofit of the housing originally designed for the EMR943C S1 class multiplier phototube. The additional length of this modified housing is required to completely enclose the new integrated system within the temperature stabilized volume. The modified housing is illustrated in Fig. 3-4. A modification to the standard temperature control housing for the incorporation of a fail safe, cutoff thermostat was initiated between the SEMINOLE (Jan 74) and SEEKVAL (Jul 74) deployments. This modification has subsequently been retrofitted to all S-20 class housings, and is to be included in all future new or retrofitted S-1 class housings.

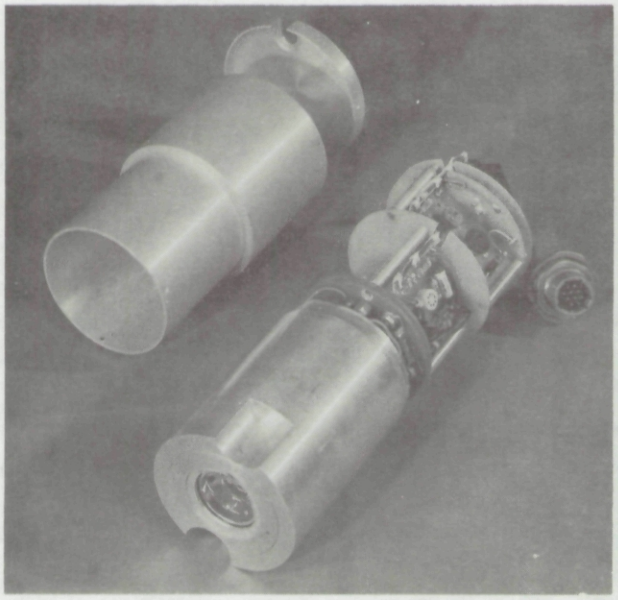

Fig. 3-3. Visibility Laboratory Integrated Radiation Detection Assembly.

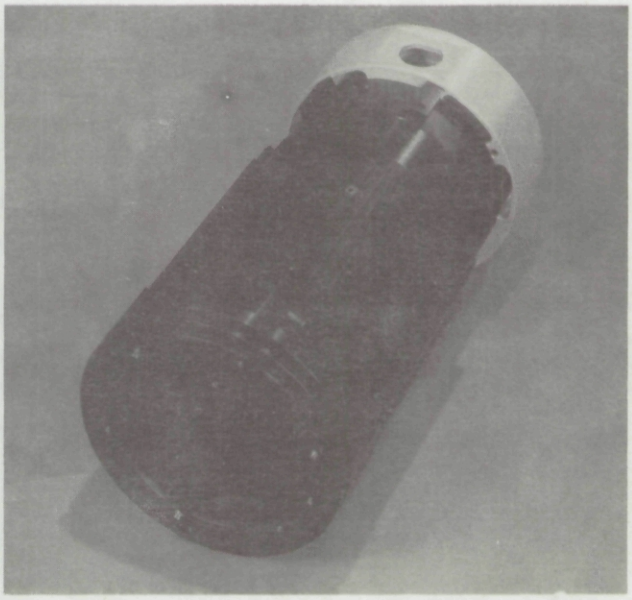

Fig. 3-4. Temperature Control Housing Assembly.

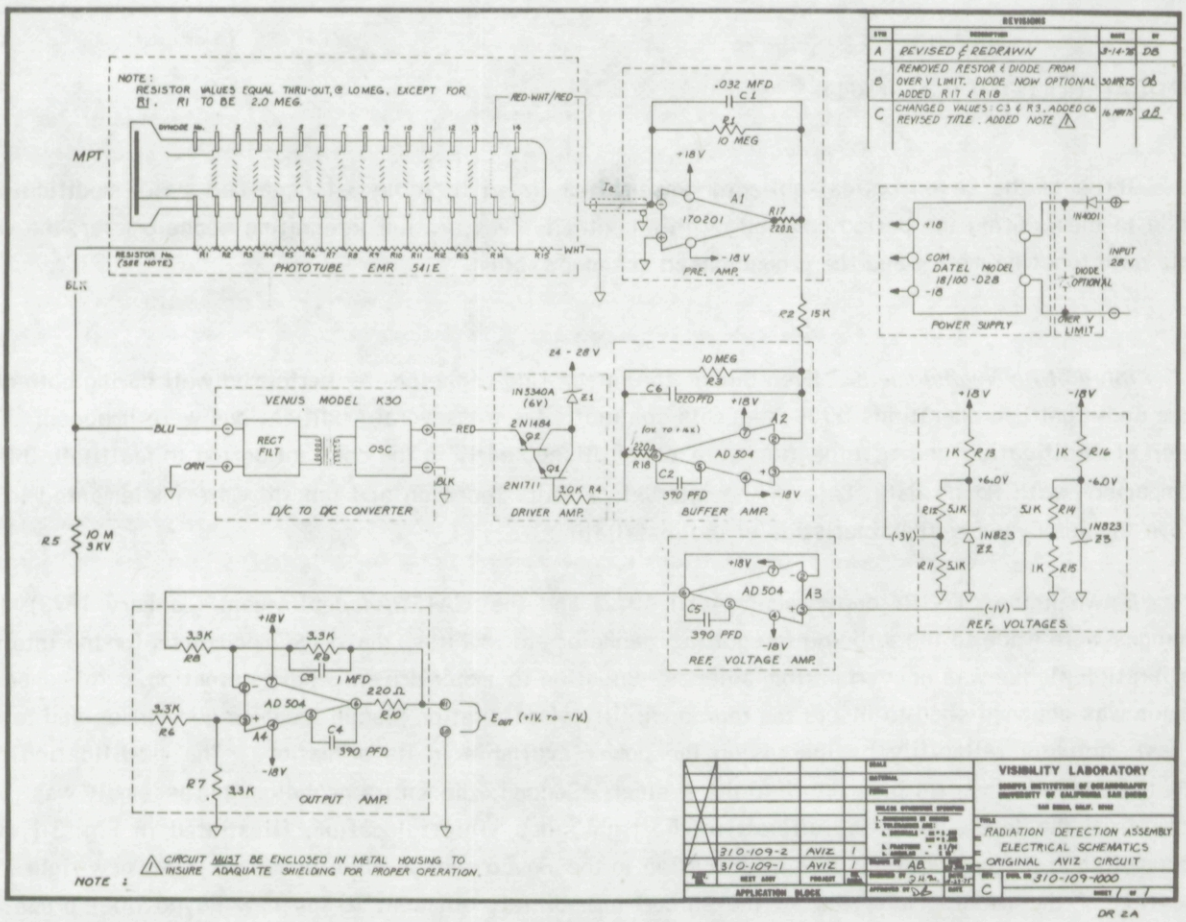

Fig. 3-5. Visibility Laboratory Radiation Detection Assembly Electrical Schematic.

OPTICAL FILTER ASSEMBLY

No modifications were made to the optical filter assemblies during this contract interval. However, there are two design changes which are recommended in the interests of improved system performance.

First, the rotary solenoids which actuate the filter holders should be replaced. As they get older they begin to lose their pull-in torque, and their return springs weaken. Both of these features tend to degrade the positional reliability and reproducibility of both the optical filters and the MEMORY mirror, resulting in instabilities in the steady-state photometer signals. The recommended modification is to replace the six solenoids per unit with a single stepper motor and geneva-driven cam assembly.

Second, the MEMORY flux is not adequately trapped during the interval when the MEMORY mirror is in the "Out" position. Consequently, during some low flux-level measurements when the radiometer is in its highest sensitivity configuration, an undesirable biasing signal is produced by the stray MEMORY flux. The recommended modification is to replace the rotating MEMORY mirror with a mechanically fixed mirror and mechanical cutoff shutter.

Both of these recommended modifications are appropriate for retrofitting into the basic housing of the existing six-flag filter changer.

OPTICAL COLLECTOR ASSEMBLIES

Three of the seven optical collector assemblies listed in Table 3-1 have had major modifications made to them during the period covered by this contract. They are the integrating nephelometer, the variable path function meter, and the ground-based scanner system.

Integrating Nephelometer. Even though the integrating nephelometer performed well during both daytime and nighttime operations throughout this contract interval, several modifications were imposed. One internal modification and a relocation were accomplished early in the contract period to facilitate intercomparison with Royco data. Late in the interval, a major redesign and rebuild were implemented to improve the aerodynamic characteristics of the installation.

Between the SENTRY deployment (April 1972) and the GATEWAY deployment (January 1973), two changes were made to the airborne integrating nephelometer. First, the drive mechanism for the internal calibration plaque was converted from solenoid actuation to motor-driven geneva actuation. This modification was accomplished to insure the reproducibility of calibration plaque location geometries and to increase actuator reliability by increasing the power available in its actuation. The modification has functioned well since its insertion into the system. Second, the entire nephelometer assembly was relocated from the left side of the aircraft to the right side. This relocation, illustrated in Fig. 3-1, was accomplished in conjunction with a modification to the Royco system inlet plumbing. The new right-side location of the nephelometer placed the shroud immediately adjacent to the new Royco inlet probe. An additional purpose for the relocation was to improve topside accessibility via the forward crew hatch.

At the conclusion of the SEEKVAL deployment (July 1974), a ruling was issued by the Air Force which declared the airborne integrating nephelometer installation inadequately documented and grounded the system from further flight. After several months of discussions it was decided to reconfigure the airborne nephelometer so that it could be enclosed within a standard C-130H type upper radome as described in Lockheed Georgia drawing number 369639, dated 1 April 1964. By April 1975 a revised, folded path configuration was devised for the nephelometer which met the mechanical constraints imposed by the radome inner dimensions, and the redesign and refabrication task was begun.

In order to fully exploit the aerodynamic shrouding provided by the modified radome, the upper hemisphere scanner and camera systems were relocated and became integral subassemblies of the new nephelometer frame and shroud. The revised configuration for this composite system is illustrated in Fig. 3-6.

The new nephelometer assembly utilizes the same basic projector and mode selector head assemblies which were reported in AFCRL-70-0137, Duntley, *et al.* (1970), Fig. 3-8, 3-9, and 3-10 and AFCRL-72-0593, Duntley, *et al.* (1972c). The difference is that the projector beam has been optically folded by inserting a front surface plane mirror into the beam between the projector and the beginning of the scattering volume. The mirror is mounted so that the angles of incidence and reflection of the projector beam are 13 degrees. Flight test for this modified installation is currently scheduled for early 1976.

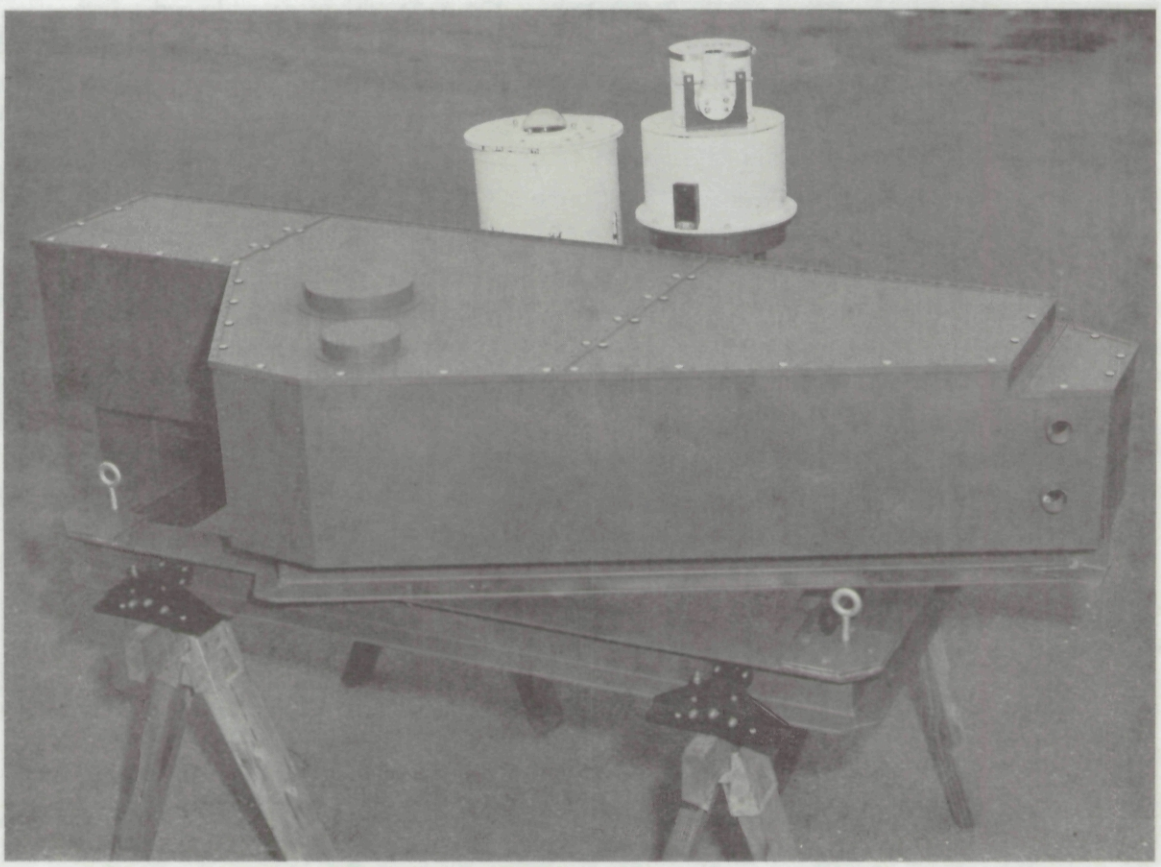

Fig. 3-6. New Folded Path Integrating Nephelometer Assembly.

Between the GATEWAY (January 1973) and HAVEN VIEW II (May 1973) deployments, the ground-based integrating nephelometer had its inlet and exhaust plumbing modified to allow increased cleaning capability and to generate an internal flow pattern more nearly colinear with the optical axis of the projector beam. This modification was implemented after a series of Royco aerosol measurements within the ground shroud indicated several eddy points at which inadequate flushing of the sample volume was occurring. Subsequent to this modification, Royco tests indicated an improved flow through the chamber; however, further evaluation and development of a flow monitoring system is recommended.

Variable Path Function Meter Assembly. The basic configuration of the airborne variable path function meter (VPFM) was fully described in AFCRL-70-0137, Duntley, *et al.* (1970), Fig. 3-14, and AFCRL-72-0593, Duntley, *et al.* (1972c), Fig. 3-4. Only two additional modifications to this experimental system have been accomplished during this contract interval, one mechanical and one optical.

The mechanical modification was accomplished specifically for the SEEKVAL deployment (July 1974). In its original configuration, the airborne variable path function meter was designed to sweep its line of sight through the forward hemisphere, i.e., from zenith angle 0 degree, down through zenith angle 90 degrees in the direction of flight, and then on down to zenith angle 180 degrees. For the SEEKVAL deployment, this particular sweep pattern was altered so that the instrument line of sight could sweep through the lower hemisphere, i.e., from dead ahead at zenith angle 90 degrees, down through the nadir point at zenith angle 180 degrees, to dead aft at zenith angle 90 degrees. The modification was accomplished by relocating the cutoff microswitches on the main shaft of the VPFM drive assembly and by mounting the yoke assembly rotated 90 degrees from its original position. The modification was simple and direct. The resulting electromechanical operation was reliable and as anticipated.

During the preliminary analysis of selected flight data from the 1973–1974 deployments it became apparent that the variable path function meter was not performing as well as it should. After extensive laboratory tests on the demounted system, it was determined that the basic design fault was related to interior baffle placement and an improper surface treatment. By November 1974, sufficient experimental evidence had been accumulated to specify a design change. A new light trap configuration was then specified and the original glossy black interior surfaces were refinished with a matt black. This revised configuration is also scheduled for flight test in early 1976.

Based on a growing need to use ground-based data either independently or in conjunction with airborne measurements, the design and fabrication of a ground-based variable path function meter was specified for completion during the contract year July 1974 – June 1975. This ground-based system was designed to be as compatible with the airborne system as possible, maintaining both optical and mechanical equivalence. The system illustrated in Fig. 3-7 was first demonstrated in February 1975 and, after several minor modifications and additions, was delivered in June 1975.

The ground-based variable path function meter incorporates several system improvements developed since the airborne model was first built:

I. It uses a built-in eyepiece and reticle for optically aligning the telescope and sunshade.

II. It utilizes an improved swivel mount for mechanically adjusting the alignment.

III. It utilizes the improved light trap discussed in the preceding paragraphs.

IV. It utilizes the new integrated radiometer circuit discussed earlier in this section.

As a result of these improved features, the ground-based variable path function meter should develop into a reliable and efficient addition to the ground-based radiometric data station.

Automatic 2π Scanner Assembly. The automatic 2π scanner assemblies are used with both airborne and ground-based instrument systems and are well-documented in AFCRL-70-0137, Duntley, *et al.* (1970), Fig. 3-6, 3-7, 3-8, as well as in AFCRL-72-0593, Duntley, *et al.* (1972c), Fig. 3-2. No significant modifications to the airborne scanners were made during this contract interval; however, two important changes were made related to the ground-based scanners.

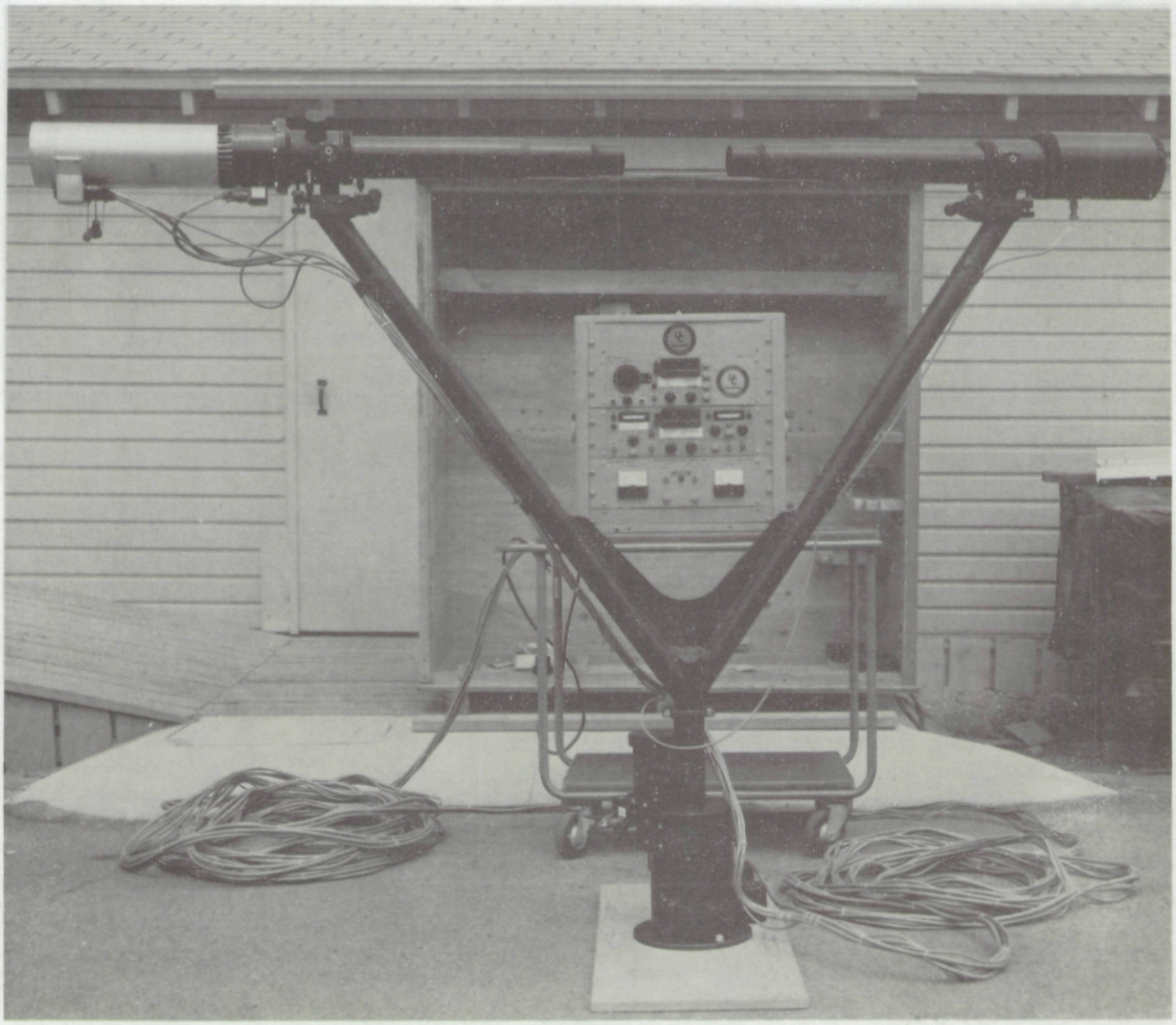

Fig. 3-7. Ground-Based Variable Path Function Meter.

The first modification was made during the period between Project GATEWAY (January 1973) and Project HAVEN VIEW II (May 1973). Prior to this time the ground-based data station optionally utilized two independent 2π scanner assemblies, one for measuring the upper hemisphere and one for measuring the lower hemisphere. The procedure was similar to that used on the airborne system. However, since the ground-based data logger is so slow, i.e., eight samples per second, the scanner data were taken sequentially, upper then lower, not simultaneously. Since the ground data were recorded one scanner at a time, it would have been advantageous to use the same detector assembly for both upper and lower hemisphere radiance measurements. In this manner, all cross-calibration problems between the two data sets would have been minimized. However, the mechanical transfer of the detector assembly from one scanner to the other would not be a trivial manipulation. Thus, an adapter block was built to join the two scanners together, and to enable the selection of either optical channel electrically.

The adapter block used to join the two scanners was a modification of the dual irradiometer prism assembly. The dual irradiometer prism assembly is illustrated in AFCRL-70-0137, Duntley, *et al.* (1970), Fig. 3-12 and 3-12A. Thus, with the new hybrid system, the operator can remotely select either the upper or lower hemisphere scanner as the optical collector for the jointly-used detector assembly. This dual scanner assembly not only reduces cross-calibration problems, but materially increases the overall procedural efficiencies of the ground team. The dual scanner assembly is illustrated in Fig. 3-8.

The chief disadvantage to the dual scanner assembly is its weight. Since the entire device weighs approximately 130 pounds, it is difficult for the ground team to orient and level the system during preliminary field setups. In an effort to simplify these preliminary procedures, a double gimbal mount was built for the dual scanner assembly. This mounting device was first utilized during the SEEKVAL deployment (July 1974) and is illustrated in Fig. 3-9. It is anticipated that this type of mounting will continue to be used with the dual scanner system, since it is an essential feature in a fully automatic remote scanner station.

3.2 METEOROLOGICAL SYSTEMS

Two modifications to the meteorological systems were completed during this contract interval.

ROYCO MODEL 220 PARTICLE COUNTER

A new plumbing installation, begun during the preceding contract interval, was completed between the SENTRY deployment (April 1972) and the GATEWAY deployment (January 1973). This plumbing simplification was discussed briefly in AFCRL-72-0593, Duntley, *et al.* (1972c). The new external probe assembly is visible in Fig. 3-1 of this report.

CAMBRIDGE MODEL 137-C3 AIRCRAFT HYGROMETER SYSTEM

The modification to this system was also begun during the previous contract interval. It was discussed and illustrated in AFCRL-72-0593, Duntley, *et al.* (1972c), Fig. 3-5. Since the completion of this modification, the Cambridge system has performed in keeping with its design specification.

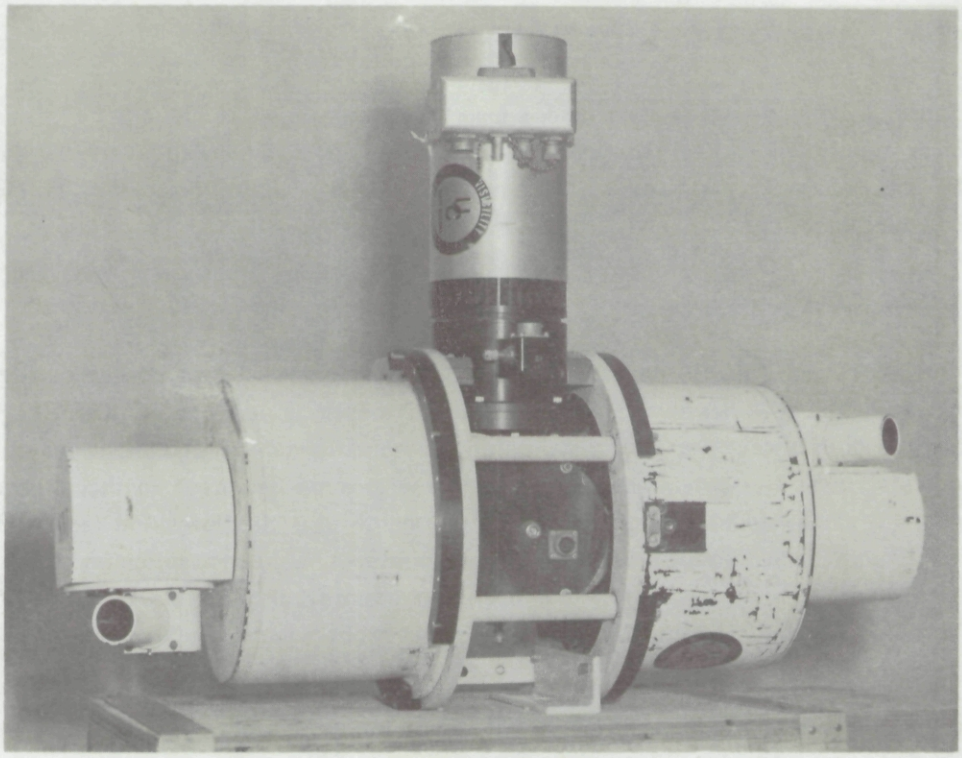

Fig. 3-8. Ground-Based Dual Scanner Assembly.

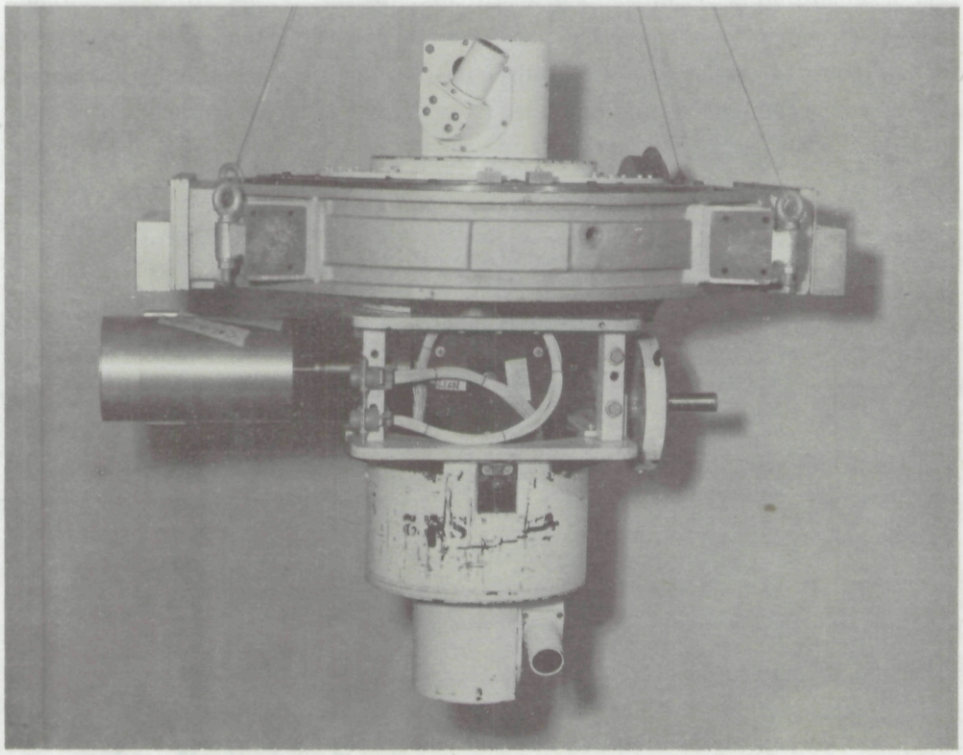

Fig. 3-9. Ground-Based Dual Scanner with Gimbal Mount.

3.3 CONTROL AND COMMUNICATION SYSTEMS

The control panels, consoles, and other support facilities listed in Table 3-1 are described along with their most significant earlier modifications in AFCRL-70-0137 and AFCRL-72-0593, Duntley, *et al.* (1970 and 1972c). Only minor additional modifications have been made to these items during the contract interval covered by this report.

PITCH AND ROLL INDICATOR

Prior to the HAVEN VIEW II (May 1973) deployment, the standard data collection flight profile included "straight and level" elements in which the aircraft was trimmed to maintain a 0-degree pitch angle. The purpose of this maneuver was to maintain a horizontal base plane for the upper and lower hemisphere scanners. There were, however, two severe shortcomings involved in this procedure. First, maintaining this flight attitude required an excessive degree of flap depression (approximately 60 degrees), which in turn caused both an exceptionally high rate of fuel consumption and a severe strain on the airframe. Second, precise orientation of the aircraft was difficult and time consuming for the pilots since there is no precision pitch indicator available on the flight console.

In order to eliminate the problems summarized above, two adjustments were made. First, mechanical shims were added to the scanner and camera mounting rings so that the base planes would be horizontal when the aircraft was in a 2½ degree nose-high attitude. Second, a digital readout was provided on the flight deck which allowed the pilot to monitor the project pitch and roll channels. This readout channel has a precision of 40 millivolts per degree and a full scale reading of 999 millivolts. Thus, to set up at 2½ degrees nose high, the pilot merely trims the aircraft until he reads +100 millivolts on the digital meter, and we are ready to go. For this slightly nose-high attitude, about only 25 degrees of flaps are normally required, which results in significant savings in fuel and the attendant increase in available data time.

42 CHANNEL DATA LOGGER

The 42 channel airborne data logger was modified just prior to the SEEKVAL deployment (July 1974) by installing new reference voltage supplies and correcting an internal grounding problem. This modification increased both the quality and current capacity of the internal calibration sources, as well as provided additional current capacity for supplying the external transducers. This modification is one in an ongoing series which involves the replacement of old custom-built subassemblies with new and commercially available substitutes. This replacement process, though sometimes expensive, is essential in order to maintain system quality and field serviceability.

3.4 PHOTOGRAPHIC SYSTEMS

Only one modification has been made to the airborne photographic system since the system was first reported and updated in AFCRL-72-0461 and AFCRL-72-0593, Duntley, *et al.* (1972b and 1972c).

The modification was accomplished between the HAVEN VIEW II deployment (May 1973) and the SEMINOLE deployment (January 1974). It involved rebuilding the Automax G-1 camera case lens cover so that it could be removed for cleaning without having to demount the camera case from the aircraft. This was a mechanically simple modification which resulted in a major saving in maintenance and servicing time. The modified camera housing is illustrated in Fig. 3-10.

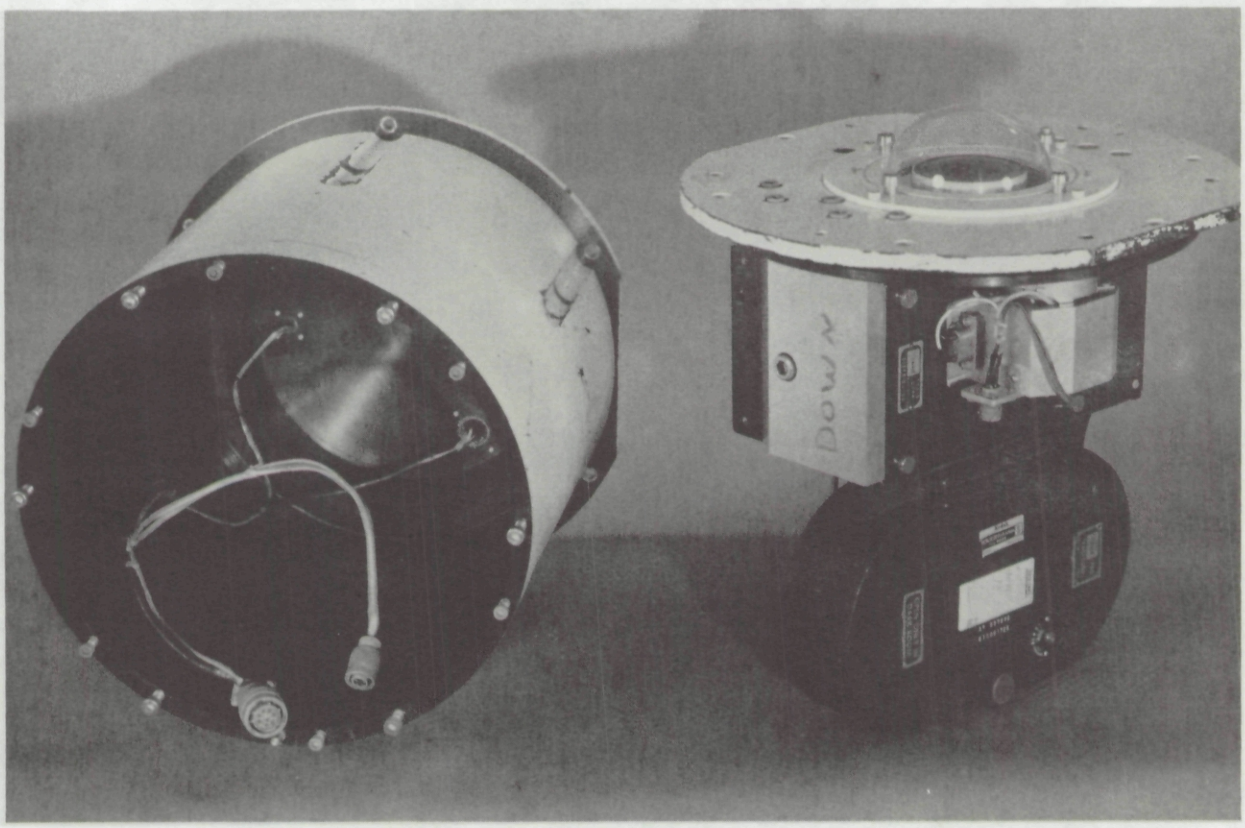

Fig. 3-10. Modified Automax G-1 Camera Case.

4. DATA COLLECTION METHODS

During this contract interval, two independent data-gathering activities were maintained simultaneously. The airborne instrument system was one activity, and the ground-based instrument system was the other. The basic concept of each experimental sequence was built around the joint operation of these two systems in a highly coordinated and simultaneous measurement routine. The procedural routine during each deployment was for each system to run full data collection sequences at every opportunity, on a daily schedule. If for any reason the joint sequences were aborted, both systems were to automatically revert to independent operation. Partial data sets were thus often obtained even when the inevitable exigencies of joint field operations defeated the basic routine. The general procedures followed by the airborne and ground-based teams are well-documented in Duntley, *et al.* (1970, 1972a and b, 1973, 1974, and 1975). Only a few comments regarding specific variations in the procedural priorities seem appropriate at this time, and they are contained in the following paragraphs.

4.1 AIRBORNE SYSTEM

The airborne data collection was accomplished through the use of an instrumented C-130A aircraft in a manner similar to that reported by Duntley, *et al.* (1970, 1972a and b, 1973, 1974, and 1975). During each data collection flight, the aircraft flew a predetermined pattern within the specified test area. An illustration of a typical flight pattern is shown in Fig. 4-1. In this stylized pattern, two basic elements, the "straight and level" and the "vertical profile," are combined to yield the total mission flight plan. A more detailed description of all flight pattern elements is presented in the above referenced reports.

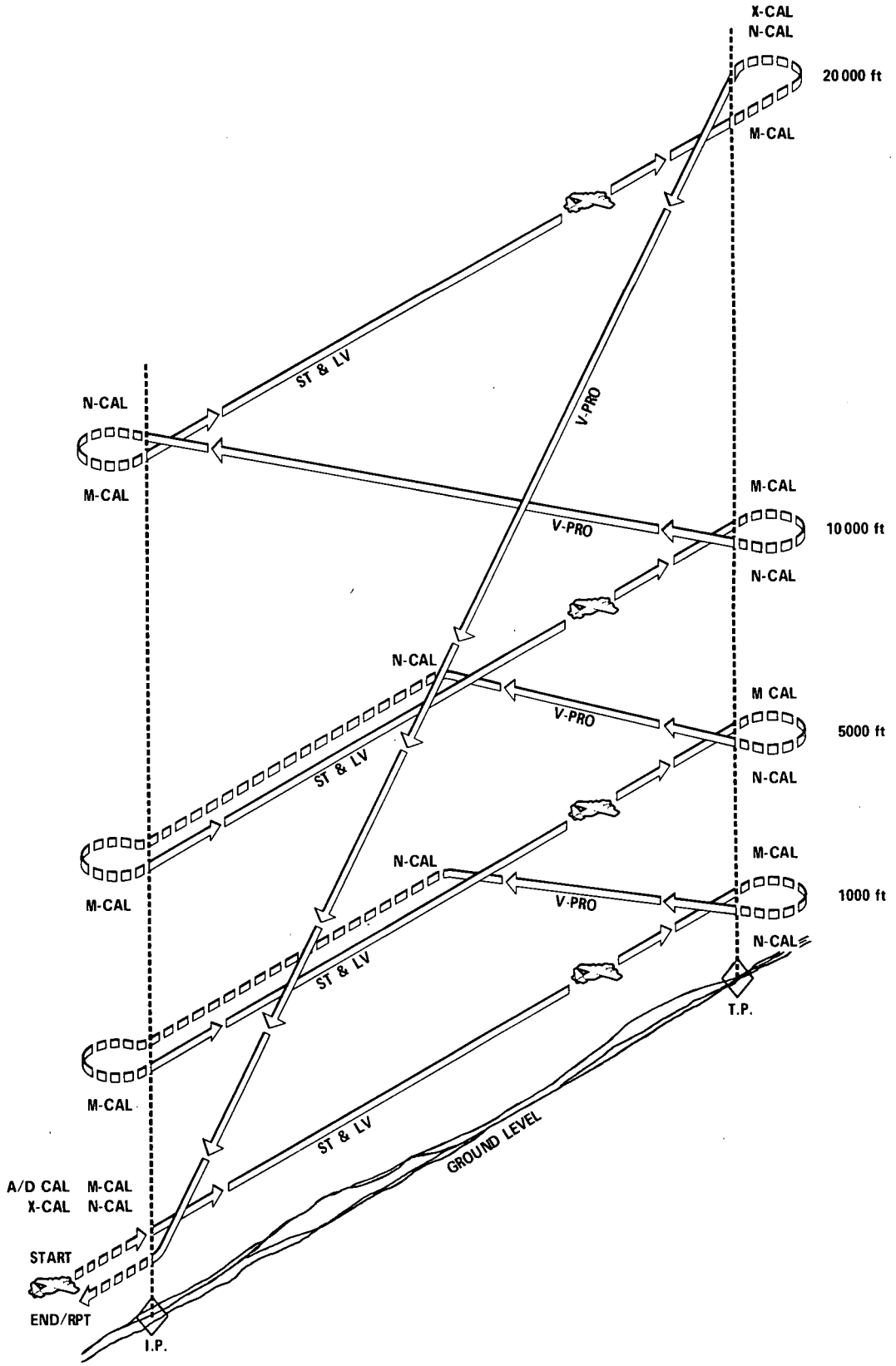

Fig. 4-1. Typical Visibility Laboratory Flight Profile.

However, in general, the data collection sequence for the airborne system has historically been broken into five standardized elements: (1) preflight warmup and calibration check, (2) straight and level sequences (ST & LV), (3) vertical profile sequences (V-PRO), (4) in-flight calibration checks (M-CAL and N-CAL), and (5) postflight calibration check. During any specific deployment, the flight profile is customized by making minor variations in the accomplishment of these five elements.

The flight profile illustrated in Fig. 4-1 represents a minor but important procedural change from the profiles illustrated in earlier reports. Prior to the HAVEN VIEW II deployment (May 1973), the standard data profile was designated a "(4 + 4)" profile. The (4 + 4) designation describes the character of the straight and level flight sequence. In this case, it means running four consecutive data sequences at each ST & LV altitude, one in each of four spectral bands, and repeating these data collection sequences at four different altitudes.

Unfortunately, a (4 + 4) profile takes approximately 4 hours to complete. Consequently, the time/space separation between the individual spectral flight elements, i.e., the Filter 2 portions of each ST & LV element and the connecting Filter 2 V-PRO element, the individual Filter 3 elements, etc., was much too extreme. To compensate for this, compromises had been gradually built into our data processing and evaluation techniques which had themselves, in our belief, begun to mask the true character of the sample aerosol and its lighting geometry. Additionally, the total elapsed time necessary for the (4 + 4) profile prohibited its use during unstable weather conditions, or whenever long ferry times were required.

As a result of these considerations, during the HAVEN VIEW II deployment (May 1973) the standard profile was changed to a "(2 + 4);" i.e., data were collected in only two spectral filters during each ST & LV element. This procedural change shortened both the length of flight track necessary and the profile elapsed time, since we achieved a considerable saving in "dead head" time. A (2 + 4) profile can be run in approximately 1 hour and 45 minutes. Thus, the sky radiance maps for each of the two filters and their associated scattering coefficient profiles are much less apt to be adversely influenced by changing sun angles and local weather disturbances. When weather conditions permit, two consecutive (2 + 4) profiles are flown back to back yielding the same data set as the original (4 + 4), but with the data within each pair of spectral bands much more closely related. The (2 + 4) profile appears to be a significant move toward achieving realistically synoptic documentation of the test site environment.

The most common variation to the flight pattern shown in Fig. 4-1 is an alteration in the altitude increments. This is done to accommodate changes in local weather conditions and/or special requirements dictated by the specific problem for which the data are being gathered. As an example, for the data reported in AFCRL-70-0137, Duntley, *et al.* (1970), the flight pattern was flown at night with five straight and level passes made between the ground and 1500 meters (5000 feet) above the ground; however, for the data reported in AFCRL-TR-74-0298, Duntley, *et al.* (1974), the flight pattern was adjusted to be flown in the daytime with three straight and level passes made between the ground and 3000 meters (10 000 feet) above the ground.

A brief summary of the data flights made during this contract interval and using the general procedures discussed in Section 4.1 is presented in Table 1-1. A more complete review of the data flights is presented in Section 6.

4.2 GROUND-BASED SYSTEM

The ground-based data collection sequence was designed to supplement the airborne data whenever the aircraft was operating in the immediate vicinity. However, it is also complete enough to stand alone when the aircraft mission is diverted or aborted. The general operating procedures have been described in the references noted in Section 4.1.

The ground-based instrument system has several operational responsibilities. First, it must supply a ground-level data base to allow interpolation of various measurements between ground altitude and the lowest attainable aircraft altitude. Second, it must supply long term temporal sampling of those meteorological and radiometric quantities which relate to the project task. Third, the ground system serves as a spare parts and repair facility for the entire air/ground operation. In the event of a catastrophic failure in a primary airborne instrument or assembly, the equivalent piece of instrumentation is reassigned to the aircraft from the ground-based system. The aircraft can then return to service with a minimum of "down-time," and repairs can be accomplished under the more convenient ground station conditions.

No major variations in ground-based procedures have been instituted during this contract interval that would alter the basic priorities presented in AFCRL-72-0593, Duntley, *et al.* (1972c). However, the specific data logging sequences have been altered slightly to be more compatible with the philosophy of the (2 + 4) airborne data sequence. Thus, ground-based measurements of earth-to-space beam transmittance in the immediate vicinity of the flight track and measurements of ground-level scattering coefficients still receive top priority. Backing up these activities and still of significant importance are the measurements of inherent terrain reflectance and clear-day sky radiance maps for the computation of earth-to-space beam transmittance.

5. DATA PROCESSING TECHNIQUE

As in any reasonably complex, multi-input sampled data system, there is a large amount of data handling required before the scientific analyst ever sees the package. The degree of data processing sophistication utilized during this contract interval is illustrated in Fig. 5-1 and 5-2. In these generalized flow charts, the basic functional steps utilized in the data processing of the raw field data are clearly specified. They do not illustrate, however, all of the miscellaneous routines used for data base management and special diagnostic purposes. A more complete description of each phase of the processing sequence is contained in AFCRL-72-0255 and AFCRL-72-0593, Duntley, *et al.* (1972a and c).

Faced with the familiar problems of an increasing data backlog and additional interpretive demands without a comparable increase in available budget, it became imperative that inefficiencies in the software flow be eliminated. The procedural approach was to treat each data flight as an independent data set and to process it in a highly stylized and routine manner. As a result of this approach, the data analyst has been able to relegate a large portion of the data diagnostic tests to automatic or semi-automatic techniques, thus freeing himself for more creative interpretive efforts. The iterative nature of this stylized approach to data processing provides an additional benefit to the analyst. The repeating format rapidly focuses his attention on procedural inefficiencies allowing prompt implementation of system improvements. With the continuing growth of the basic data bank, there is continuing incentive to convert the remaining manual procedures to automatic. These conversions, though somewhat expensive to implement, yield substantial increases in data-handling reliability and automatic diagnostic capability.

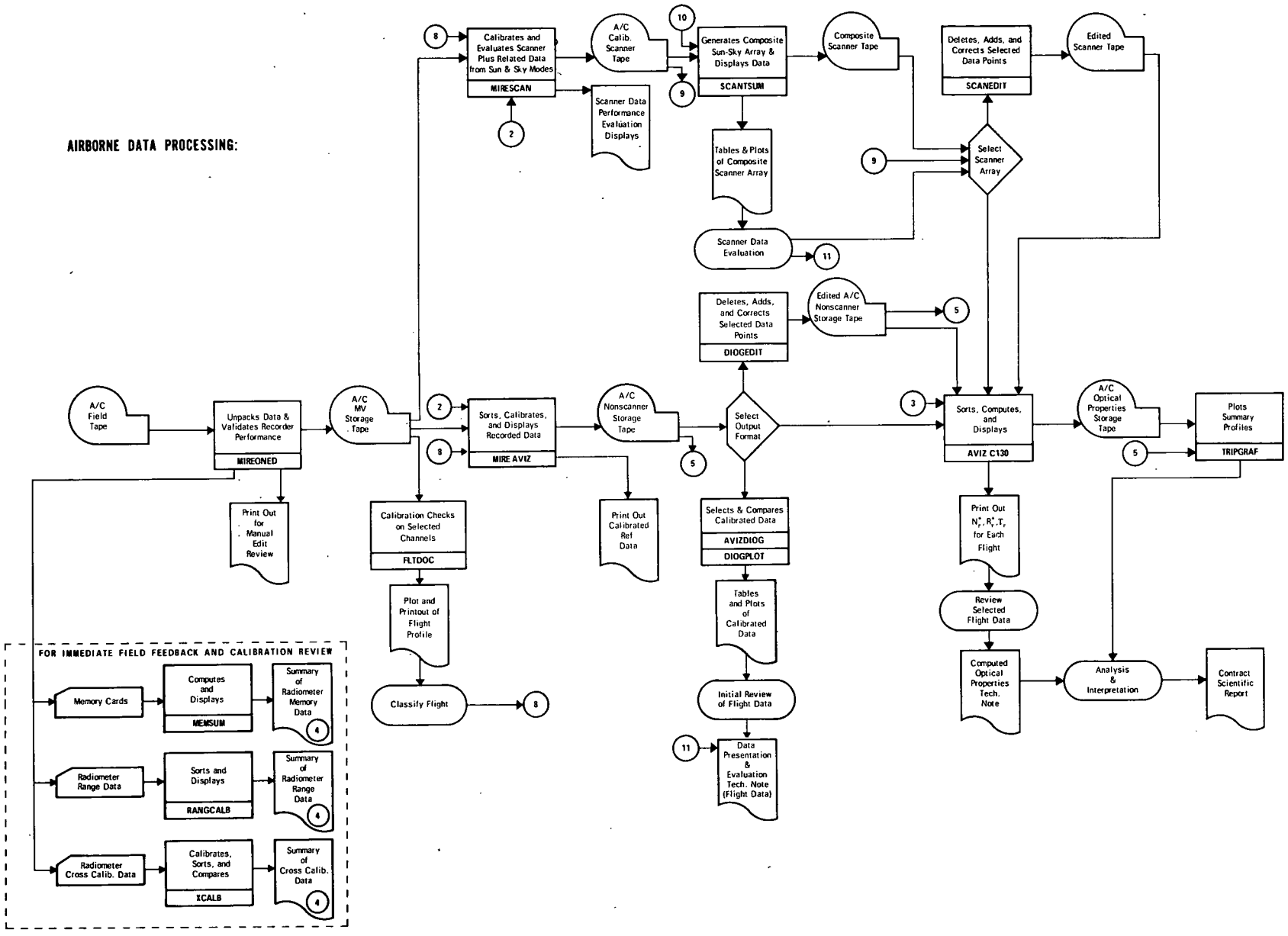

Fig. 5-1. Atmospheric Visibility Program Data Processing Schedule, Airborne Data.

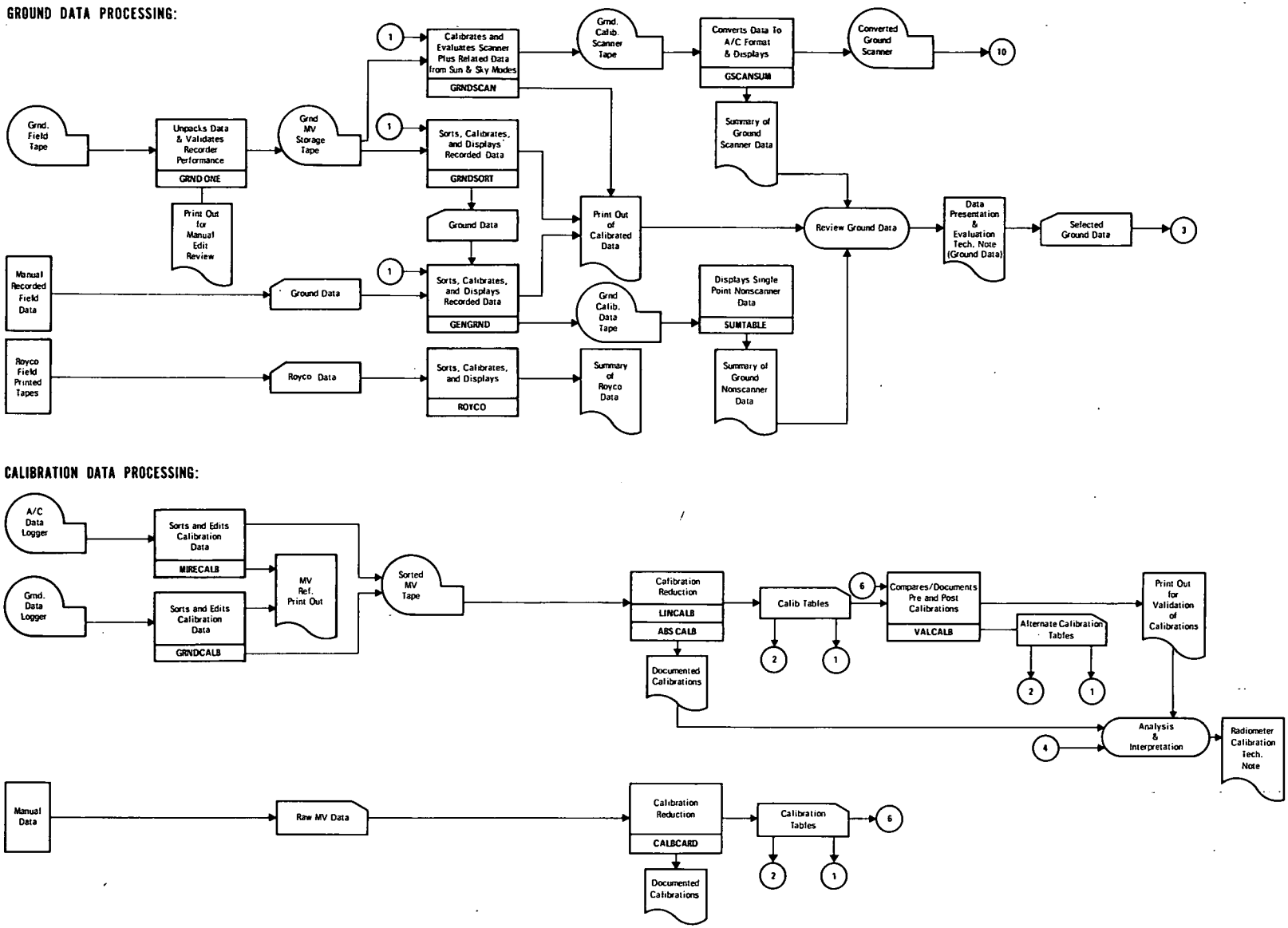

Fig. 5-2. Atmospheric Visibility Program Data Processing Schedule, Ground-Based and Calibration Data.

During the contract interval covered by this report, the major software effort was in the development and efficient implementation of the new procedures illustrated in Fig. 5-1 and 5-2. The specific emphasis on the data processing development has been twofold: directed first at isolating the automatic scanner data and streamlining the procedure of converting the measured field data directly into report format, and second, at developing an automatically documented data bank so that additional analysis using computer methods could readily be undertaken. The use of the technical documentation procedure described in AFCRL-72-0593, Duntley, *et al.* (1972c), has worked effectively in recording data quality. The use of standard identification codes on project computerized data banks has greatly facilitated the automatic storage and retrieval procedures necessary for efficient data handling.

AIRBORNE DATA

In order to speed up the initial validation of field data, an additional step in the early processing of the flight data was incorporated into the schedule illustrated in Fig. 5-1. This step was designed to check and display the output of each system mode or orientation identification channel. A preliminary look at these selected control signals provides an increased degree of confidence in predicting the successful, or unsuccessful, completion of the automatic calibration and display phase. Program FLTDOC was developed to display graphically each of the flight elements (ST & LV, V-PRO, etc.) based upon its recorded identification code, and to list for each of these elements the appropriate mode or orientation information. These displays permit quick classification of the flight's data segments into sets which are processable and correspond to the parts of the standard profile described in Section 4. This early classification of the flight data permits very selective processing which provides the analyst with both an adequate representation of the flight's overall quality and the ability to exercise close control of processing economies.

A large effort has been expended directly on handling the airborne scanner data during this contract interval. With the advent of the nonspiral mode of scanner data collection in 1972, it became desirable to split the airborne data processing into two basic parts, scanner and nonscanner data. Program MIRESCAN was developed for processing, as a unit, all of the data directly related to the automatic 2π scanner system. Its primary function is to calibrate and sort the scanner data into a standardized array whose azimuthal axis is oriented with respect to the major light source, the sun or the moon. This standardized array is maintained, in terms of format, throughout all subsequent data manipulations. Thus a high degree of compatibility among software packages is maintained throughout all subsequent analysis stages.

Following the initiation of the sun/sky mode of data collection in 1972, increased sophistication was required in the scanner data processing schedule. The in-flight measurement of selected sky radiances in both high and low sensitivity ranges called for additional software development to combine these redundant measurements into the standard array. Program SCANTSUM was developed to generate this composite array. This composite data array represents a fully "on-scale" 2π steradian map of the upper hemisphere radiance distribution. All points within the composite array, including those near the sun, fall within the calibrated radiometric span of either the sky mode or sun mode measurements, a feature that did not exist in earlier procedures. As a further diagnostic aid, Program SCANTSUM provides both tabular and graphical displays of all three data sets of near sun data, i.e., the sky mode measurements near the sun, the sun mode measurements near the sun, and the resultant composite measurements near the sun.

As the processing of a particular set of flight data progresses, the interim determinations of the analyst plus the vagaries of complex machine operations soon beget a multiplicity of computer reruns. As the number of reruns increases, the more important it becomes to have a fully documented procedure for identifying each run and any data base alteration it may have performed. The computer accomplishes this documentation automatically by labeling each program run with a unique job number and date, as well as the equivalent identifying labels for the run's input data base. Thus the labeling system enables the analyst to trace all data manipulations step by step from any point in the procedure back to the initial calibration of the flight tape.

All program runs for a specific flight are segregated in a chronological file, affording automatic documentation of all work performed by the computer on each data set. This automatic documentation is an important feature for a small staff operation since it allows each person to concentrate on analysis instead of using his or her time in the bookkeeping task of manually documenting what has been done to the data by each pass through the computer.

After a set of flight data completes its course through the schedule illustrated in Fig. 5-1, it is stored in a stylized data bank. The latest data files from each flight for which computed optical properties have been generated are combined into one of three project review files: one for scanner data, one for nonscanner data, and one for the resultant computed optical properties generated for the flight. These files form the basic computerized data bank for each flight and, collectively, for each deployment set.

Selected backup files are also retained in a composite file for use in the generation of supplementary data, or the regeneration of replacement files as the occasion demands.

GROUND-BASED DATA

The initial requirement to combine both manually and magnetically recorded data from the ground-based systems has led to the use of a card-oriented system for the first stage of processing. This procedure is illustrated in Fig. 5-2. The card input capability has also facilitated the correction of errors resulting from intermittent data logger problems. The basic field data is composited onto tape for processing in the calibration and display phases.

The only exception to the card-oriented input is the handling of the ground-based scanner data. Scanner data is retained on tape throughout the processing because of the quantity involved. Since the ground scanner may be oriented in various mechanical positions, the format for handling its data is often altered for each deployment. The scanner operates in a manner similar to the airborne system; however, because of the difference in recorder rates, the quantity of data derived from the ground system is less than from the airborne counterpart. Therefore, the ground scanner data is interpolated into the same standard format as is used to store aircraft scanner data by Program GSCANSUM. This format can then be handled by the same software used on the aircraft data. This interface between the ground scanner data and the aircraft scanner standard array was not completed until late in the contract interval. However, its recent insertion into the software system has provided another extremely useful and productive tool to the data analyst.

6. DATA ACQUISITION SUMMARY

6.1 FIELD TRIP SUMMARY

The data acquired during the 3-year contract period were primarily daytime airborne measurements. Four field trips were made between January 1973 and July 1974 and a total of 48 flights made. The locations, dates, and flights for each of the field trips are presented in Table 6-1. When dates are given without flight numbers, the reference is to the ground station site and the number of ground data sets. Flight numbers which are not listed were assigned to flights during which no optical data were taken.

Table 6-1. Field Trip Summary

Field Trip	Geographic Location	Track or Site Reference	Latitude	Longitude	Ground Elevation (meters)	Begin	End	Flight No.	Total No. Flights or Ground Sets
GATEWAY	Southern Illinois	Track 3 Vandalia	39.4° N	88.8° W	183	13 Jan 73	31 Jan 73	250 , 251 254B, 255A	4
		Track 7 Maples	37.8° N	91.5° W	305	13 Jan 73	31 Jan 73	252 , 253 254A, 255B	4
		Shelby County Airport	39.4° N	88.8° W	188	12 Jan 73	27 Jan 73	–	10
HAVEN VIEW II	Northern Germany	Lathen-Oldenberg	53.0° N	07.7° E	21	12 May 73	15 Jun 73	270 to 290	21
		Meppen Test Range	52.9° N	07.3° E	18	9 May 73	11 Jun 73	–	21
SEMINOLE	Western Florida	Panama City	29.9° N	86.2 W	0	17 Jan 74	9 Feb 74	300 to 308	9
		Eglin Aux No. 1	30.6° N	86.3° W	30	11 Feb 74	12 Feb 74	309, 310	2
		Mexico Beach	29.9° N	85.4° W	7	15 Jan 74	13 Feb 74	–	20
SEEKVAL	Western Washington	Rainier	46.9° N	122.7° W	158	12 Jul 74	28 Jul 74	350 to 360	11
		Rainier	46.9° N	122.7° W	158	12 Jul 74	29 Jul 74	–	13

6.2 DESCRIPTION OF FIELD TRIPS

GATEWAY

The GATEWAY field trip to southern Illinois encompassed 24 days in January and February 1973. During this interval, the aircraft, operating out of Scott Air Force Base, flew seven daytime data collection missions. The ground station, operating near Shelbyville, Illinois, at the Shelby County Airport, collected a total of 10 assorted data sets on 6 separate days. The ground station consisted of the flyaway contrast reduction meter kit only. Flight track locations are illustrated in Fig. 6-1.

The GATEWAY deployment was the first field trip during which the integrating nephelometer was mounted on the right-hand side of the aircraft. It was also the first field use of the revised Royco inlet plumbing and updated Cambridge hygrometer probe.

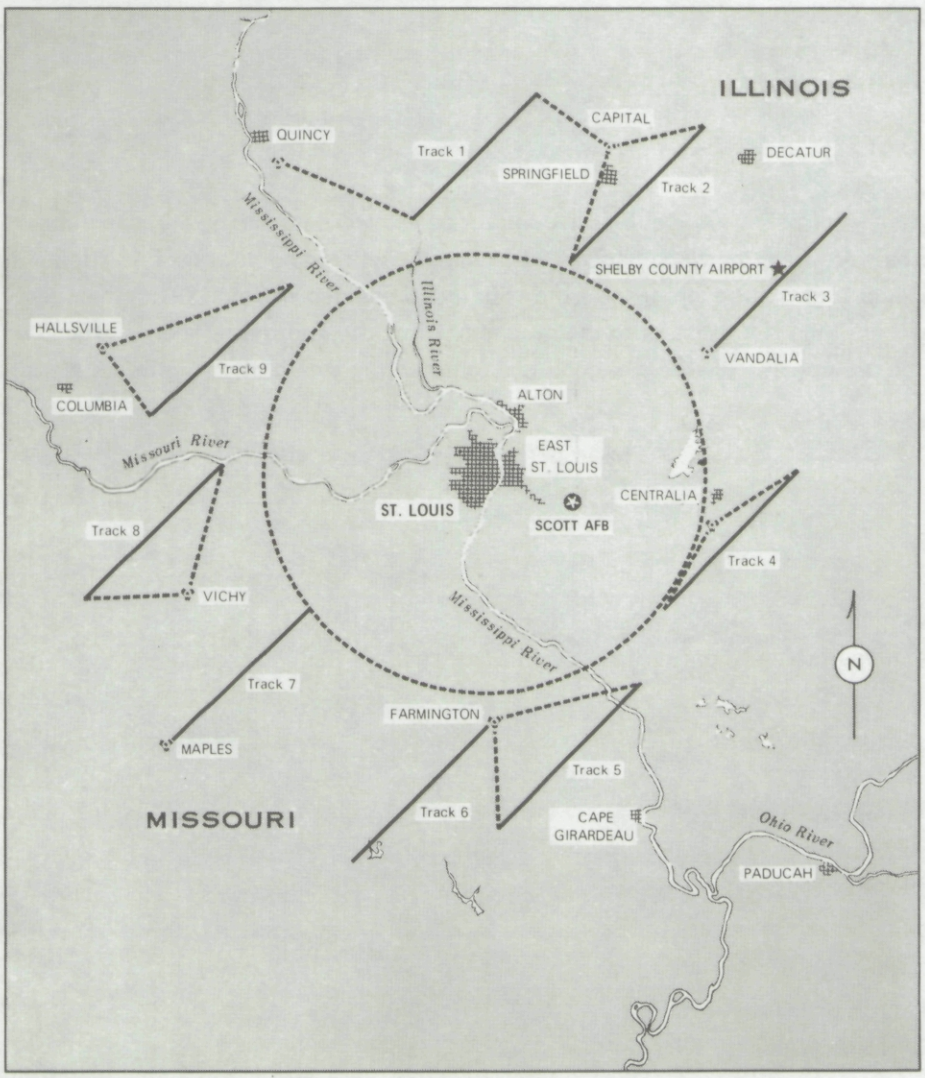

Fig. 6-1. Typical GATEWAY Flight Tracks.

Weather hampered the flight schedule during this deployment with widespread precipitation accompanying and following frontal pasages.

The track 3 flights were conducted over typically flat terrain consisting mostly of harvested winter farmlands. There were intermittent patches of snow and many frozen ponds and streams.

The track 7 flights were conducted over typically wooded rolling hills. The woods were barren, brown, and interspersed with patches of light snow.

HAVEN VIEW II

The HAVEN VIEW II field trip to northern Germany encompassed 58 days in May and June 1973. During this interval, the aircraft, operating out of Wunstorf Air base and Rhein-Main Air Base, flew 21 daytime data collection missions. The ground station, operating near Meppen, Germany, collected a total of 21 assorted data sets on 19 separate days. The ground station consisted of the fully equipped instrument van illustrated in Fig. 3-2. Flight track locations are illustrated in Fig. 6-2.

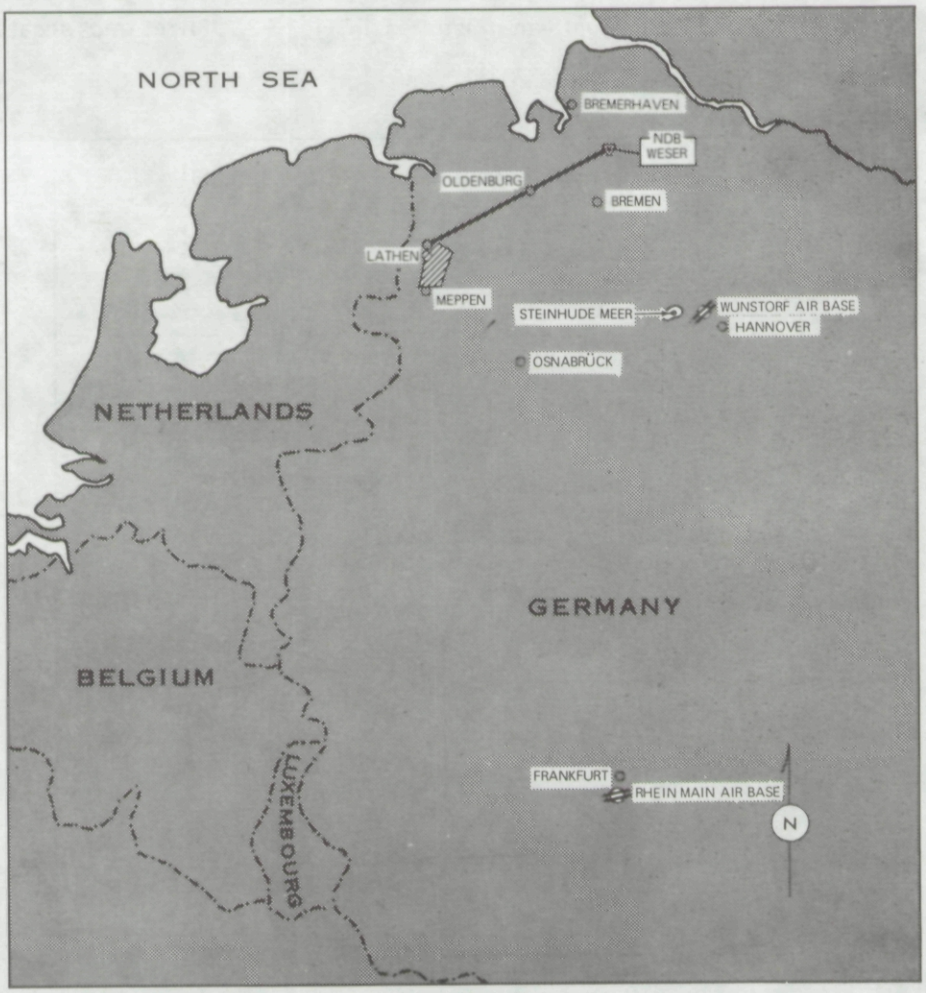

Fig. 6-2. Typical HAVEN VIEW II Flight Tracks.

The HAVEN VIEW II deployment was the first field trip to utilize the digital pitch and roll readout on the flight deck. It was also the first field use of the ground-based dual scanner assembly.

It should be recognized that HAVEN VIEW II was not conceived as being a fair-weather mission, and "clear-day" data will be available in very limited quantity. However, the cloudy, hazy, and overcast conditions which were encountered are typical of a large portion of the real world's weather pattern and should be included in both our inventory of data and processing capabilities.

All flights were conducted over low-lying flat terrain consisting mostly of cultivated farmland interspersed with dark patches of dense woods.

SEMINOLE

The SEMINOLE field trip to western Florida encompassed 34 days in January and February 1974. During this interval, the aircraft, operating out of Eglin Air Force Base, flew seven daytime and four nighttime data collection missions. The ground station, operating near Mexico Beach, Florida, collected 10 assorted data sets on 10 separate days and 10 assorted data sets on 8 separate nights. The ground station consisted of the fully equipped instrument van illustrated in Fig. 3-2. Flight track locations are illustrated in Fig. 6-3.

Fig. 6-3. Typical SEMINOLE Flight Tracks.

The SEMINOLE deployment was the first field trip for which the aircraft system utilized external power supplies for all three photometer reference voltages.

Cloudy weather was typical for most flights during this deployment, whether they were day or night missions. All but the last two flights were over the ocean with generally calm water conditions prevailing.

SEEKVAL

The SEEKVAL field trip to western Washington encompassed 24 days in July 1974. During this interval, the aircraft, operating out of McChord Air Force Base, flew 11 daytime data collection missions. The ground station, operating near Rainier, Washington, collected 13 assorted data sets on 13 different days. The ground station consisted of the fully equipped instrument van illustrated in Fig. 3-2. Flight track locations are illustrated in Fig. 6-4.

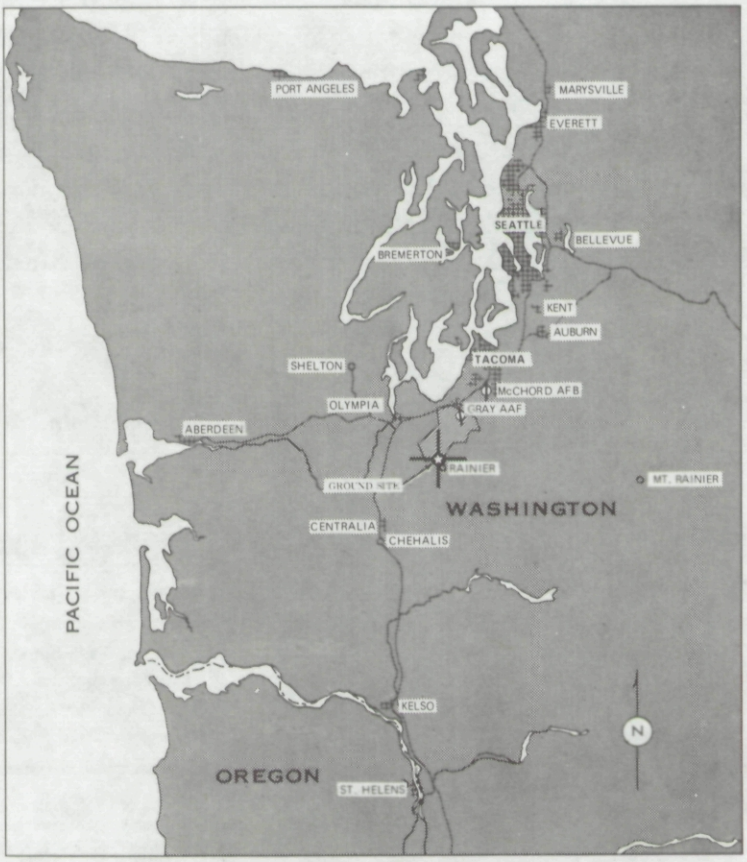

Fig. 6-4. Typical SEEKVAL Flight Tracks.

The SEEKVAL deployment was the first field trip to use the variable path function meter modified to sweep through the lower hemisphere with its line of sight, i.e., from $\theta = 90°$ forward to $\theta = 90°$ aft. It was also the first airborne test of the integrated radiometer circuit and the first ground-based use of the dual scanner gimbal mount.

Cloudy or overcast weather was typical for this deployment; however, 3 of the 11 data flights are classified as basically clear-day situations.

The SEEKVAL flight profiles were not the typical (2 + 4) as discussed in Section 4.1. They were a special mix of ST & LV elements and V-PRO elements selected primarily to yield a broad variety of photographic data. The radiometric measurements were intermixed with a series of photographic runs in an attempt to provide equivalent sets of photographic and radiometric data suitable for subsequent cross-comparisons. During these missions radiometric measurements were made in the pseudo-photopic spectral band only. All flights were conducted over a flat grassy prairie surrounded with broad expanses of dark evergreen woods.

6.3 DATA BANK SUMMARY

The nine field trips described in AFCRL-72-0593, Duntley, *et al.* (1972c), plus the four described in Section 6.2 immediately preceeding, provide a data bank which can be used to derive atmospheric optical properties for the downward path of sight. An initial sorting of the flight data has been made to determine the number of flights which are sufficiently complete to warrant further processing. Data for three straight and level altitude runs plus the vertical profile data in each of three filters is the minimum requirement except for special-purpose missions like SEEKVAL. Of a total of 50 flights during this contract period, 43 are complete. When these flights are added to those from the previous contract, the total accumulated data bank consists of 107 flights. A summary of these flights, sorted by latitude, is presented in Table 6-2 with the season and terrain briefly described.

Table 6-2. Available Data Bank of Daytime Data

Latitude	Season	Terrain	Field Trip	Geographical Location	No. Complete Flights
53° N	May, Jun	Green pasture	HAVEN VIEW II	Northern Germany	18
48° N	May, Jun	Green pasture	HAVEN VIEW I	Southern Germany	10
46.9° N	Jul	Brown prairie	SEEKVAL	Western Washington	10
45.5° N	Mar.	Snow, ice	SNOWBIRD	Northern Michigan	4
43.3° N	Apr	Rolling hills, wooded	SENTRY	New Hampshire	8
41.5° N	Apr, May	Dry range	HAVEN VIEW I	Northern Spain	2
38.5° N	Apr	Ocean	HAVEN VIEW I	Western Mediterranean	4
38.5° N	Aug	Cultivated farm	METRO	Southern Illinois	14
38.5° N	Jan	Cultivated farm	GATEWAY	Southern Illinois	6
35.0° N	Jan	Desert	LOCAL III	Southern California	3
33.5° N	May	High desert	HAVEN VIEW I	Eastern Morocco	3
33.3° N	Oct, Nov	High desert	ATOM	Central New Mexico	7
33.2° N	Mar.	Low desert	LOCAL I	Southern California	2
33.2° N	Oct	Low desert	LOCAL II	Southern California	1
33.2° N	Jan, Feb	Low desert	LOCAL III	Southern California	2
32.7° N	Mar., Apr	Ocean	LOCAL I	Southern California	2
–	Oct	Ocean	LOCAL II	Southern California	1
–	Feb	Ocean	LOCAL III	Southern California	1
29.9° N	Jan, Feb	Ocean	SEMINOLE	Western Florida	9

7. PROJECTION & RECOMMENDATIONS

As an outgrowth of the experience and expertise gained during the analysis and evaluation of the data gathered during this contract interval, several potentially powerful techniques have been developed, and numerous improvements to procedural and computational efficiencies have been accomplished. Some further comment related to these techniques and how they might influence the goals of the technical program is summarized in the following paragraphs.

PROJECTION

Significant gains have been made in processing and reporting the data during this contract interval which have greatly improved the accessibility of the data in the growing data bank.

Calibrations Processed.. All the radiometer calibrations for the data bank listed in Table 6-2 have now been processed and analyzed. Calibration data for the last two field trips were processed within 3 to 4 months of the conclusion of the trip. In addition during this contract interval, the calibration data were processed for all of the remaining unreported field trips from preceding contract intervals. Thus all radiometric data in the bank now have useable and readily accessible calibration data stored on tape. It is expected that radiometer calibration processing and analysis will be routinely completed within 1 to 2 months after each ensuing field trip.

Flight Data Reported. Both the number of flights reported and the ratio of flights reported to flights acquired have increased during this contract interval. Data for 22 flights were reported during this contract period, and data for 43 flights were acquired. This is compared to data for only 12 flights reported versus data for 64 flights acquired during the first contract interval.

The interval between data acquisition and report issuance has also been diminished. The latest scientific report followed the field trip by 1 year versus 2 to 3 years for the previous reports. This was in spite of the fact that many computer processing procedures had to be modified to accommodate the scanner array pattern change and the addition of sun mode data.

It is projected that an increasingly larger proportion of the developing data bank will be reported in the ensuing contract period, assuming adequate funding.

RECOMMENDATIONS

Path Function Measurements. Diagnostic tests applied to the variable path function meter data for the flights reported in AFCRL-TR-75-0414, Duntley, *et al.* (1975a) indicated valid measurements were being obtained in contrast to the earlier abnormally high values induced by stray light within the instrument. In addition, a ground-based variable path function meter was completed in June 1975 which measures directly a variable that has hitherto been available only through calculation. It is recommended that emphasis be put on flight and field tests of these two instruments and that cross-comparisons then be made to other data and computed values.

Scattering Function Recovery. The endeavor to develop the method of scattering function recovery described in Section 2.1 should continue. Up to this point, the attempts have principally involved earlier data with less reliable radiance gradient information near the sun. Only one of the flights with sun mode data reported in AFCRL-TR-75-0414, Duntley, *et al.* (1975a) could be used for this purpose; the rest were either lacking in scattering function values at 30 and 150 degrees or not sufficiently clear of clouds. This one flight had a span of sun zenith angle from 67 to 35 degrees. In general, primary emphasis should be put on the use of large sun zenith angle data during the development of the recovery method. The large sun zenith angle data provide effective equilibrium radiance for a large range of scattering angles thus deemphasizing the method of extrapolating the effective equilibrium radiance to a scattering angle of 180 degrees.

Non-Rayleigh Model Atmospheres. Efforts should continue to calculate atmospheric optical properties using the Gordon (1969) model atmosphere equations with the Barteneva (1960) proportional directional scattering functions as described in Section 2.2. In this way the expected range in values of given variables can be established as well as the inter-relationships between various parameters. The computer program for evaluating the model atmosphere equations is both fast and inexpensive. Nineteen combinations of vertical beam transmittance and proportional directional scattering function were selected as appropriate for evaluation. Of these, the calculations for eight have been completed. Effort should be made to complete the remaining 11 cases so that full evaluation and utilization of the results can be made.

1964 Ground-Based Data from Automatic Instruments. The ground-based data from the beam transmissometer, sky scanner, and irradiometer mounted on a rooftop of the Visibility Laboratory during 1964 should be fully exploited. This unique set of data is comprised of values of apparent sun radiance, solar aureole radiance, downwelling irradiance, and sky radiance for a wide range of solar zenith angles from winter through summer. One major use of the data is to provide a sizeable catalog of values of vertical earth-to-space transmittance, path radiance, and path reflectance. In addition, comparisons can be made between measured downwelling irradiance and computed downwelling irradiance, where the computed values are derived from measurements of sky radiance, irradiance, and atmospheric beam transmittance. The portion of the data from cloud-free days could be used to further validate the method of obtaining beam transmittance from sky radiance ratios. Finally, the large sun zenith angle data near 80 degrees could be utilized to help develop the method of scattering function recovery.

Cloudy-Day Techniques. As the total number of data flights increases, a larger and larger sample of days having marginal to poor flying conditions is being accumulated. Since the cloudy, hazy, and broken overcast conditions which typify these days constitute a large portion of the real world's weather pattern, the optical atmospheric properties associated with these conditions are as critically needed, or even more so, as are the properties associated with clear days. It is recommended that an increased effort be made to adapt the experimental and computational techniques used so successfully under fair weather stable illumination levels to the much more difficult experimental situation of poor weather with unstable illumination levels.

Climatological Relationships. A continuing goal of the Visibility Laboratory's measurement program is the accumulation of a body of data appropriate for direct application to the interpretation of the relationship between the optical properties of the atmosphere and the meteorological specifications of that atmosphere. With the extensive optical properties data bank now becoming available, it seems logical to approach the problem of defining the geographical area over which each particular set of optical properties is probably valid. An experimental flight profile designed to monitor optical properties over an elongated, fixed altitude track, traversing a well-defined meteorological reporting net would be an attractive first step. If reasonably defined optical transitions can be determined, then the corollary variations in the meteorological descriptions may become more readily identifiable. Using these experimental results as a guide, the effort to identify the areas of highest correlation between our optical properties data base and other existing climatological data bases should begin to yield increasingly useful results.

8. ACKNOWLEDGEMENTS

To be conducted successfully, a research program such as the one reported herein requires the active support of many organizations and individuals. To all of those who so willingly contributed their skills, talents, and inspiration, the authors gratefully acknowledge their debt.

Dr. Robert W. Fenn, Chief, Atmospheric Optics Branch, AFCRL,
Scientific Counsel and Technical Monitor
Lt. Col. Aaron B. Loggins, USAF, Project Organization and Coordination
Major Robert W. Endlich, USAF, Project Organization and Coordination
Mr. Raymond S. Silva, Operational Services Division, Field Requirements Section
AFCRL, for continuing logistical support and advice

3245th ABGp., Hanscom AFB, MA & 4900th Test Group, Kirtland AFB, NM
(for all aircrew assignments)

Visibility Laboratory, Technical Field Team:
Mr. J. Douglas Bailey, ground station crew
Mr. George F. Simas, ground station crew
Mr. Leonard A. Castro, technical flight crew
Mr. Robert L. Stapleford, technical flight crew
Mr. Gerald D. Edwards, ground station crew

Visibility Laboratory, Data Processing and Analysis Team:

Mr. Nils R. Persson, Jr.
Ms. Janet E. Shields
Ms. Catharine F. Edgerton
Ms. Carolyn M. Williams
Mr. Steven J. Bettinger

Visibility Laboratory, Editorial and Reproduction Team:

Ms. Sally L. Poor
Mr. John C. Brown
Ms. Arlene C. Streed
Mr. James Rodriguez
Ms. Alicia G. Enriquez

9. REFERENCES

Barteneva, O. D. (1960), "Scattering Functions of Light in the Atmospheric Boundary Layer," Bull. Acad. Sci. U.S.S.R., Geophysics Series, 1237–1244.

Boileau, A. R. (1968a), "Atmospheric Optical Measurements in the Vicinity of Crater Lake, Oregon, Part I." University of California, San Diego, Scripps Institution of Oceanography, Visibility Laboratory, SIO Ref. 68-18.

Boileau, A. R. (1968b), "Atmospheric Optical Measurements in the Vicinity of Crater Lake, Oregon, Part II." University of California, San Diego, Scripps Institution of Oceanography, Visibility Laboratory, SIO Ref. 68-19.

Boileau, A. R. (1968c), "Atmospheric Optical Measurements in Central Colorado in Connection with Long Range Oblique Photography," Applied Optics, **7**, 407–414.

Brown, D. R. E. (1952), *Natural Illumination Charts,* Report 374-1, Project Ns-714-100, Department of the Navy, Bureau of Ships, Washington, D. C.

Coulson, K. L., J. V. Dave, and Z. Sekara (1960), *Tables Related to Radiation Emerging from a Planetary Atmosphere with Rayleigh Scattering,* University of California Press.

Duntley, S. Q., A. R. Boileau, and R. W. Preisendorfer (1957), "Image Transmission by the Troposphere I," Journal of the Optical Society of America **47**, 499–506.

Duntley, S. Q., R. W. Johnson, and J. I. Gordon (1964), "Ground-Based Measurements of Earth-to-Space Beam Transmittance, Path Radiance, and Contrast Transmittance," University of California, San Diego, Scripps Institution of Oceanography, Tech. Doc. Rep. AL-TDR-64-245.

Duntley, S. Q., R. W. Austin, J. H. Taylor, and J. L. Harris (1966), "Visual Acuity and Astronaut Visibility," University of California, San Diego, Scripps Institution of Oceanography, Visibility Laboratory, SIO Ref. 66-17.

Duntley, S. Q., R. W. Austin, J. L. Harris, and J. H. Taylor (1968), "Experiments on Visual Acuity and the Visibility Markings on the Ground in Long Duration Earth-Orbital Space Flight," University of California, San Diego, Scripps Institution of Oceanography, Visibility Laboratory, SIO Ref. 68-6, also published by NASA, Washington, D. C. as NASA-CR-1134 (1968).

Duntley, S. Q. (1969), "Directional Reflectance of Atmospheric Paths of Sight," Duntley Rep. No. 69-1.

Duntley, S. Q., R. W. Johnson, J. I. Gordon, and A. R. Boileau (1970), "Airborne Measurements of Optical Atmospheric Properties at Night," University of California, San Diego, Scripps Institution of Oceanography, Visibility Laboratory, SIO Ref. 70-7, AFCRL-70-0137.

Duntley, S. Q., R. W. Johnson, and J. I. Gordon (1972a), "Airborne Measurements of Optical Atmospheric Properties in Southern Germany," University of California, San Diego, Scripps Institution of Oceanography, Visibility Laboratory, SIO Ref. 72-64, AFCRL-72-0255.

Duntley, S. Q., R. W. Johnson, and J. I. Gordon (1972b), "Airborne and Ground-Based Measurements of Optical Atmospheric Properties in Central New Mexico," University of California, San Diego, Scripps Institution of Oceanography, Visibility Laboratory, SIO Ref. 72-71, AFCRL-72-0461.

Duntley, S. Q., R. W. Johnson, and J. I. Gordon (1972c), "Airborne Measurements of Optical Atmospheric Properties, Summary and Review," University of California, San Diego, Scripps Institution of Oceanography, Visibility Laboratory, SIO Ref. 72-82, AFCRL-72-0593.

Duntley, S. Q., R. W. Johnson, and J. I. Gordon (1973), "Airborne Measurements of Optical Atmospheric Properties in Southern Illinois," University of California, San Diego, Scripps Institution of Oceanography, Visibility Laboratory, SIO Ref. 73-24, AFCRL-TR-73-0422.

Duntley, S. Q., R. W. Johnson, and J. I. Gordon (1974), "Airborne and Ground-Based Measurements of Optical Atmospheric Properties in Southern Illinois," University of California, San Diego, Scripps Institution of Oceanography, Visibility Laboratory, SIO Ref. 74-25, AFCRL-TR-74-0298.

Duntley, S. Q., R. W. Johnson, and J. I. Gordon (1975a), "Airborne Measurements of Optical Atmospheric Properties in Western Washington," University of California, San Diego, Scripps Institution of Oceanography, Visibility Laboratory, SIO Ref. 75-24, AFCRL-TR-75-0414.

Edgerton, C. F. (1967), "Relationship between Meteorological Conditions and Optical Properties of the Atmosphere," University of California, San Diego, Scripps Institution of Oceanography, Visibility Laboratory, SIO Ref. 67-27.

Gordon, J. I. (1963), "Predictions of Sighting Range Based Upon Measurements of Target and Environmental Properties," University of California, San Diego, Scripps Institution of Oceanography, Visibility Laboratory, SIO Ref. 63-23.

Gordon, J. I. (1969), "Model for a Clear Atmosphere," J. Opt. Soc. Am. **59**, 14–18.

Gordon, J. I., J. L. Harris, and S. Q. Duntley (1973), "Measuring Earth-to-Space Contrast Transmittance from Ground Stations," Applied Optics **12**, 1317–1324.

Gordon, J. I., C. F. Edgerton, and S. Q. Duntley (1975), "Signal-Light Nomogram," J. Opt. Soc. Am. **65**, 111–118.

Hulburt, E. O. (1957), "Measurements and Estimates of Sky Brightness for All Altitudes of the Sun for Various Altitudes of the Observer Above the Surface of the Earth," Naval Research Laboratory, Washington, D. C., NRL Report 4870.

Johnson, F. S. (1954), "The Solar Constant," Journal of Meteorology **11**, 431–439.

Kasten, F. (1965), "A New Table and Approximation Formula for the Relative Optical Airmass," Arch. Met. Geophys. Bioklim. **B14**, 206–233.

Preisendorfer, R. W. (1958), "Theory of Attenuation Measurements in Planetary Atmospheres," University of California, San Diego, Scripps Institution of Oceanography, Visibility Laboratory, SIO Ref. 58-81.

Pyaskovskaya-Fesenkova, E. R. (1957) *Investigation of the Scattered Light in the Earth's Atmosphere,* Acad. Nauk, U.S.S.R., Moscow (in Russian) p. 182. Polar plot of data also published by N. Robinson (ed.) *Solar Radiation* Elsevener Publ. Co. Amsterdam/London/New York (1966) Figure 3.14 p. 65.

Tousey, R., and E. O. Hulburt (1947), "Brightness and Polarization of the Daylight Sky at Various Altitudes Above Sea Level," J. Opt. Soc. Am. **37**, 78–92.

Tyler, J. E. and R. W. Preisendorfer (1962), "Light," Chap. 8 in *The Sea*, M. N. Hill, Ed. (Interscience Publishers, Inc., (N.Y.), Vol. 1, pp. 397– 451.

U. S. Standard Atmosphere (1962), U. S. Government Printing Office, Washington, D. C. 20402.

☆ U. S. GOVERNMENT PRINTING OFFICE: 1976--600-223--23